

See discussions, stats, and author profiles for this publication at: <https://www.researchgate.net/publication/231706485>

Non-Centrosymmetric Lamellar Structures in the Associating Blends of Tri- and Diblock Copolymers

ARTICLE *in* MACROMOLECULES · MARCH 2010

Impact Factor: 5.8 · DOI: 10.1021/ma9023735

CITATION

1

READS

14

5 AUTHORS, INCLUDING:



Igor Erukhimovich

Lomonosov Moscow State University

100 PUBLICATIONS 1,432 CITATIONS

SEE PROFILE



Elena N. Govorun

Lomonosov Moscow State University

29 PUBLICATIONS 230 CITATIONS

SEE PROFILE



Mikhail V Tamm

Lomonosov Moscow State University

29 PUBLICATIONS 153 CITATIONS

SEE PROFILE

Non-Centrosymmetric Lamellar Structures in the Associating Blends of Tri- and Diblock Copolymers

I. Ya. Erukhimovich,^{*,†,‡} M. V. Belousov,[‡] E. N. Govorun,[‡] V. Abetz,[§] and M. V. Tamm[‡]

[†]Institute of Organoelement Compounds, RAS, Moscow 119991 Russia, [‡]Physics Department, Moscow State University, Moscow 119991 Russia, and [§]Institute of Polymer Research, GKSS Research Centre Geesthacht GmbH, 21502 Geesthacht, Germany

Received October 28, 2009; Revised Manuscript Received February 15, 2010

ABSTRACT: We consider lamellar morphologies in the mixtures of *AC* diblock and *ABC* triblock copolymers and show that a proper functionalization of the end blocks of the triblock and diblock copolymer chains by donor and acceptor functional groups, respectively, could result in occurrence of the thermodynamically stable non-centrosymmetric lamellar structures in such mixtures. Depending on the chemical nature of the donor-acceptor bond (i.e., the values of the effective entropy S_{bond} and energy E per one bond), the typical phase diagrams could contain the upper and lower triple points where the pure diblock, pure triblock and noncentrosymmetric lamellae of a finite composition coexist. With increase of the association strength the triple points merge and the noncentrosymmetric lamellae become thermodynamically favorable at all temperatures. The boundary on the (S_{bond}, E) -plane, which separates the regions corresponding to different types of the phase behavior, is found. The influence of the architecture of the system and the chemical nature of the donor-acceptor bond on the stability of the noncentrosymmetric lamellae is analyzed and typical phase diagrams are presented.

1. Introduction

Materials with a macroscopic electric polarization display a variety of useful properties, such as piezo- and pyroelectricity and second-order nonlinear optical activity. So, it has been much debated in the past two decades^{1–7} if it is possible to form noncentrosymmetric materials from molecules, which are themselves noncentrosymmetric but not chiral. R. Stadler has proposed to obtain self-assembled periodic noncentrosymmetric lamellar (NCL) structures oriented on the micrometer scale by mixing suitably chosen *ABC* triblock copolymers with *ac* diblock copolymers. Such structures were, indeed, obtained in mixtures of polystyrene-*block*-polybutadiene-*block*-poly(*tert*-butyl methacrylate) (*SBT*) triblock copolymer with a polystyrene-*block*-poly(*tert*-butyl methacrylate) (*ST*) diblock copolymer and of polybutadiene-*block*-polystyrene-*block*-poly(methyl methacrylate) (*BSM*) triblock copolymer with a polybutadiene-*block*-poly(methyl methacrylate) (*BM*) diblock copolymer.⁸ Later on, the NCL structures were obtained in a blend of two *SBT* triblock copolymers, which differed only in the length of their middle blocks.⁹ (Here and thereafter we use the capital italic letters to designate both the chemically identical repeating units we further call for brevity monomers and the blocks consisting of them. To specify whether the *blocks* do belong to the tri- or diblock copolymers we designate the blocks by the upper and lower italic case, respectively. To specify whether the chemically identical *layers* are formed of the blocks that belong to the tri- or diblock copolymers we designate the layers by the upper and lower bold case, respectively.)

The thermodynamic reasons for NCL to exist were outlined in ref 8 as follows. In linear *ABC* triblock copolymers, the simplest lamellar (smectic) mesophases consist of well-segregated layers of different monomers *A*, *B*, and *C*. Indeed, chemically different polymer species are, in general, incompatible, and segregation effects are strong. Then the energetically favored lamellar arrangement is

the centrosymmetric lamellae $(\text{ABCCBA})_n$. Compared to a non-centrosymmetric sequence $(\text{ABCABC})_n$, high-energy **AC** interfaces have been replaced by low-energy **AA** and **CC** contacts. The situation is much less trivial for lamellar structures of mixtures of triblock and diblock copolymers. Minimizing the highly-energetic interfaces between different chemical species, we are still left with three basic different types of possible arrangements shown in Figure 1.

All of them have the same number of high-energy **ac**, **AB**, **BC** interfaces between incompatible layers but differ in the number and order of the interfaces **AA**, **Aa**, **aa** (**CC**, **Cc**, **cc**) between the layers formed by the chemically identical *A*(*C*)-monomers pertaining to tri- and diblock copolymer chains. It is this difference that could be important. Indeed, the copolymer chains assembled into layers are stretched in order to minimize the interface and thus the number of contacts between unlike species. Generally, the stretching in **A**- and **a**-layers is different, as the stretching in triblocks is governed by *A*–*B* and *B*–*C* interactions rather than *A*–*C* interaction as that in diblocks. So, for the **Aa** contact, the interdigitation profile is asymmetric: the more and less strongly stretched chains invade differently the region occupied by their counterpart chains. As a consequence, the system gains energy f_A^{ex} by replacing a pair of one **AA** and one **aa** contact by two **Aa** contacts. Similar considerations apply to *C* and *c* blocks. Therefore, depending on the energies f_A^{ex} and f_C^{ex} we call further the exchange energies, different situations can occur.

Macroscopically demixed domains of centrosymmetric double bilayer $(\text{acca})_n$ and trilayer $(\text{ABCCBA})_n$ arrangements formed of pure diblock and triblock copolymers, respectively, are favored for $f_A^{\text{ex}} > 0, f_C^{\text{ex}} > 0$ (Figure 1a). Next, the centrosymmetric double pentalayer arrangements $(\text{CBAaccaABC})_n$ and $(\text{ABCcaacCBA})_n$ will be favored, respectively, for $f_A^{\text{ex}} < 0, f_C^{\text{ex}} > 0$ (Figure 1b) and $f_A^{\text{ex}} > 0, f_C^{\text{ex}} < 0$ (not shown). At last, the desired noncentrosymmetric pentalayer arrangement $(\text{ABCCa})_n$ (Figure 1c) occurs if the exchange free energy of the system favors both **aA** and **cC** interfaces ($f_A^{\text{ex}} < 0, f_C^{\text{ex}} < 0$).

*Corresponding author.

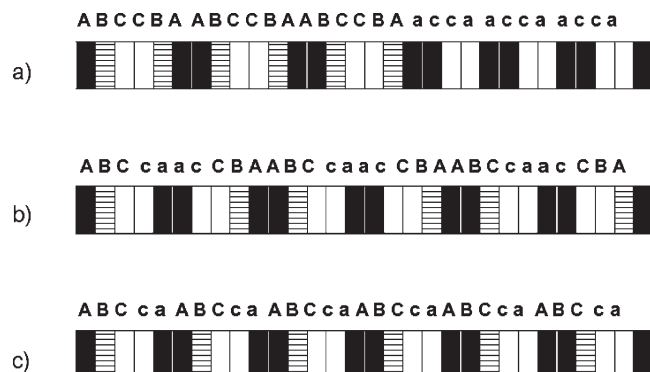


Figure 1. Three types of lamellar morphologies expected in the blends of the linear triblock *ABC* and diblock *ac* copolymers: (a) coexisting pure tri- and diblock lamellar phases; (b) centrosymmetric lamellae formed by double pentalayers **ABCcaacCBA**; (c) noncentrosymmetric lamellae formed by the pentalayers **ABCca**.

If one or both the exchange free energies would vanish, then a random sequence of pentalayers **ABCca** (**CBAac**) or trilayers **ABC** (**CBA**) and bilayers **ac** (**ca**) would be favored. However, this case is hardly observable since the actual quantity governing alternation of the bi- and trilayers is $f_{\alpha}^{\text{ex}} S$, where $\alpha = A, C$, and S is the layer interface area whose absolute value is large even if the quantity f_{α} is close to zero. Thus, in what follows we consider only the situation when $f_A^{\text{ex}}, f_C^{\text{ex}} \neq 0$.

Which of the exchange energies (if any) would be negative and, thus, which morphology actually would be formed in the mixture, depends on a subtle balance of the polymer entropic conformational effects (described above) and the energetic interactions both within and between the layers.

It follows from the discussion above that such an entropic effect is formed on scales of the order of the width D of the interpenetration zone between the chemically identical (athermal) layers, which is small as compared to the total width of the layer.^{10,11} Therefore, the effect is also small. In the case of strong segregation and purely athermal **A** and **a** layers the NCL formation may occur only in some rather special circumstances.¹¹ Moreover, within the self-consistent Scheutjens–Fleer calculations the exchange energies f_A^{ex} and f_C^{ex} are found to be always positive,¹² which corresponds, as explained above, to macrophase separation of the *ABC/ac* blend into the pure *ABC* and *ac* phases.

A study of the NCL formation in the blends of the linear triblock *ABC* and diblock *ac* copolymers within the intermediate segregation has been carried out¹³ via the self-consistent field theory (SCFT) for a rather special case when all three the Flory interaction parameters describing mutual incompatibility of the blocks are equal or almost equal:

$$\chi_{AB} = \chi_{BC} = \delta\chi_{AC} = \chi, \quad |\delta - 1| \ll 1 \quad (1.1)$$

According to phase diagrams built in ref 13, the NCL is the dominant phase in a narrow region of the blend compositions, the width of the region being rapidly decreasing with increase of χ . However, in a broad composition interval outside of the pure NCL phase stability region the blend is found¹³ to separate into the NCL and one of the almost pure block copolymer components (either *ABC* or *ac*). Unfortunately, the authors¹³ presented no discussion of the way to find the real chemical nature of the *A*, *B*, and *C* components with the χ -parameters obeying the condition in eq 1.1.

On the other hand, it has been noticed¹⁴ that the condition in eq 1.1 could correspond to the systems with specific interactions even though the effect of the latter can not be described properly by a modification of the χ -parameters only (we address this issue in more detail below). A similar hint to an explicit way to promote

the NCL formation in the *ABC/ac* blends could be extracted from the discussion above related to Figure 1. Namely, one has to search for some special ways to diminish the free energy of the neighboring **Aa** and **Cc** layers. One of the most natural choices in this direction is to use as NCL forming systems the blends of the *ABC* and *ac* block copolymers properly functionalized to provide specific interactions of donor-acceptor type between the *C* and *c* (*A* and *a*) monomers. It is to present a detailed theoretical consideration of the conditions when the NCL is formed in these systems within an extended Alexander–de Gennes (AdG) model,^{15,16} which is the purpose of our paper. We show that the proper functionalization of the blends under consideration does lead to formation of broad common layers stabilized due to donor-acceptor interaction and thus making the exchange energies f_{α} negative. We find also conditions for the degree of functionalization as well as the reduced entropy and energy of the donor-acceptor bonds which would ensure formation of the NCL lamellar morphology.

The further presentation is organized as follows. In the next section we remind the reader, following refs 15–18, how the AdG model describes formation of the lamellar structure both in pure *ac* and *ABC* melts. In section 3, we extend the AdG model to consider stability of the centrosymmetric pentalayer lamellar morphology in the *ABC/ac* mixtures with donor-acceptor interaction between the *C* and *c* blocks. The central point of section 3 is discussion of how the intralamellar specific interaction influences the equilibrium structure of the *Cc* (**Aa**) interfaces and the phase coexistence between different lamellar structures in such melts. In particular, we show here that due to association a common layer is formed of the overlapping associating blocks between (or instead of) the layers **C** and **c**. In section 4, the AdG model is extended to study stability of the noncentrosymmetric pentalayer lamellar phase in the case when both the *C*–*c* and *A*–*a* donor-acceptor interactions take place. Here we find the conditions ensuring that the noncentrosymmetric pentalayers **ABCca** become the most thermodynamically favorable. In section 5, we outline a phenomenological way to allow for the chemistry effects and carry out the topological classification of the phase diagrams of the NCL-forming system as dependent on the values of the parameters defining the donor-acceptor association between different blocks (i.e., the entropies and reduced energies of the donor-acceptor bonds). At last, in section 6, we discuss the relevance of our theoretical results to the real systems, and make some concluding remarks.

2. Alexander–de Gennes Model for Melts and Blends of Di- and Triblock Copolymers^{15–18}

2.1. Diblock Copolymer Melts. Consider first the *ac* diblock copolymer melt. In this paper we assume for simplicity that the copolymer macromolecule is not too asymmetric, in which case the melt is known to form the lamellar morphology under increase of the component incompatibility. In such melts the “building brick” is the bilayer **ac** formed by the block copolymer chains whose junction points belong to the same interface between the **c** and **a** layers. In the strong segregation limit we presume here the blocks *c* and *a* do not overlap because of their incompatibility. The blocks *a*, *a'* (*c*, *c'*) starting from the different **ac** interfaces do not overlap either to avoid an extra stretching caused by such overlapping. Then the incompressibility conditions hold:

$$\sigma_{\text{di}} h_i = n_i v_0, \quad i = a, c \quad (2.1)$$

Here $\sigma_{\text{di}} = S_{\text{di}}/M_{\text{di}}$ is the surface area per one chain (S_{di} and M_{di} being the total area of the **ac** interfaces in all bilayers and the total number of the diblock copolymer chains in the system, respectively), n_i is the number of monomers per block

of the sort i , and h_i is the width of the layer filled by such blocks. To simplify the subsequent calculations it is convenient to rewrite eq 2.1 in terms of the reduced (dimensionless) widths $H_i = h_i/l$ and specific area $\Sigma_{\text{di}} = \sigma_{\text{di}}/v_0$ (l and v_0 are the length of the statistical segment and monomer excluded volume, respectively, assumed for simplicity to be the same for A , B , and C monomers):

$$\Sigma_{\text{di}} H_i = n_i \quad (2.1a)$$

The free energy per diblock chain in such a lamellar structure is a sum of the interfacial, elastic and interaction contributions:

$$f_{\text{di}} = \sigma_{\text{di}} \gamma_{\text{di}} + f_{\text{di}}^{\text{el}} + n_a f_A + n_c f_C \quad (2.2)$$

Here f_A , f_C are the contributions into the specific (per corresponding monomer) free energies of the pure polymers due to the short-range interaction of the monomers (A and C , respectively), γ_{di} is the interfacial tension for the interface **ac** (or **Ac**, or **AC**, or **aC**), and

$$f_{\text{di}}^{\text{el}} = \frac{3T}{2} \left(\frac{H_a^2}{n_a} + \frac{H_c^2}{n_c} \right) = \frac{3T N_{\text{di}}}{2 \Sigma_{\text{di}}^2} \quad (2.3)$$

is the elastic (stretching) free energy per diblock copolymer chain. Here T is the temperature, which in this paper is measured in energetic units and $N_{\text{di}} = n_a + n_c$ is the total degree of polymerization of diblock copolymer. So, given the value of the reduced surface per chain Σ_{di} , the total free energy of the system would read

$$F_{\text{di}} = T M_{\text{di}} \left(\tilde{\gamma}_{\text{di}} \Sigma_{\text{di}} + \frac{3 N_{\text{di}}}{2 \Sigma_{\text{di}}^2} \right) + M_{\text{di}} N_{\text{di}} (x_a f_A + x_c f_C) \quad (2.4)$$

where $x_i = h_i/(h_a + h_c) = n_i/N_{\text{di}}$ ($i = a, c$), and $\tilde{\gamma}_{\text{di}} = (\gamma_{\text{di}} v_0)/(aT)$ is the reduced interfacial free energy. In fact, however, the value of Σ_{di} is not an independent variable. On the contrary, the value of Σ_{di} is self-adjustable to provide the minimum of the full free energy of the system. Minimizing the rhs of eq 2.4 with respect to Σ_{di} , one finally obtains

$$\begin{aligned} \Sigma_{\text{di}}^{\text{eq}} &= (3 N_{\text{di}} / \tilde{\gamma}_{\text{di}})^{1/3}, \\ f_{\text{di}}^{\text{eq}} &= (3T/2) (3 \tilde{\gamma}_{\text{di}}^2 N_{\text{di}})^{1/3} + N_{\text{di}} (x_a f_A + x_c f_C) \end{aligned} \quad (2.5)$$

On the other hand, the free energy of the homogeneous melt of the AC diblock copolymer is

$$F_{\text{di}}^{\text{hom}} = M_{\text{di}} N_{\text{di}} f(x_a, x_c) \quad (2.6)$$

where $f(x_a, x_c)$ is the contribution into the specific (per monomer) polymer free energy due to short-range interaction of the monomers A and C having the volume fractions x_a and x_c , respectively. (The contribution to the polymer free energy due to translation entropy of the chains could be neglected within the adopted AdG approximation.)

Thus, the total free energy of forming the lamellar structure from a homogeneous melt per chain reads

$$\begin{aligned} \Delta f_{\text{di}}^{\text{lam}} &= (3T/2) (3 \tilde{\gamma}_{\text{di}}^2 N_{\text{di}})^{1/3} + \\ N_{\text{di}} ((x_a f(1, 0) + x_c f(0, 1)) - f(x_a, x_c)) \end{aligned} \quad (2.7)$$

where we took into account that $f_A = f(1, 0)$, $f_C = f(0, 1)$. In the subsequent estimations we use the Flory–Huggins¹⁹ and

Hildebrand²⁰ approximations for $f(x_a, x_c)$:

$$f(x_a, x_c) = -(v_0/2) \sum_{i,j=A,C} \delta_i \delta_j x_i x_j \quad (2.8)$$

where δ_i is the solubility parameter of the i -th component. Then expression 2.7 takes the form

$$\begin{aligned} \Delta f_{\text{di}}^{\text{lam}} &= (3/2) (3 \tilde{\gamma}_{\text{di}}^2 N_{\text{di}})^{1/3} \\ &- (N_{\text{di}} v_0/2) ((x_a \delta_A^2 + x_c \delta_C^2) - (\delta_A x_a + \delta_C x_c)^2) \\ &= T ((3/2) (3 \tilde{\gamma}_{\text{di}}^2 N_{\text{di}})^{1/3} - \chi_{AC} N_{\text{di}} x_a x_c) \end{aligned} \quad (2.9)$$

where we introduced the Flory parameter $\chi_{AC} = v_0 (\delta_A - \delta_C)^2/(2T)$.

Next, using the Helfand–Tagami expression for the surface tension²¹

$$\gamma_{ij} = (Tl/v_0) (\chi_{ij}/6)^{1/2} \rightarrow \tilde{\gamma}_{ij} = (\chi_{ij}/6)^{1/2} \quad (2.10)$$

we get finally the excess free energy per chain of the lamellar phase as compared to the disordered state:

$$\Delta f_{\text{di}}^{\text{lam}}/T = 3 \tilde{\chi}^{1/3} / 2^{4/3} - \tilde{\chi} x_a x_c \quad (2.11)$$

As seen from 2.11, the excess free energy as a function of the reduced parameter $\tilde{\chi} = \chi_{AC} N_{\text{di}}$ increases with $\tilde{\chi}$ in the interval $0 \leq \tilde{\chi} \leq (x_a x_c)^{-3/2}/4$ and then decreases, so that the lamellar phase becomes thermodynamically advantageous as compared to the disordered one for

$$\tilde{\chi} \geq \tilde{\chi}_{tr} = (1/4) (3/x_a x_c)^{3/2} \quad (2.12)$$

For the symmetric block copolymer with $x_a = x_c = 0.5$ the value of the reduced parameter $\tilde{\chi}$ in the phase transition point $\tilde{\chi}_{tr}(0.5) = 6 \times 3^{1/2} \approx 10.392$ is remarkably close¹⁷ to that given by the strict self-consistent field consideration of Leibler.²² Of course, due to the scaling nature of the AdG approximation,²³ this fact is to be considered only as a lucky coincidence, which witnesses, anyway, that the described AdG model is a rather satisfactory estimate for the free energy of molten diblock copolymers.

2.2. Triblock Copolymer Melts. Similarly, the “building brick” of the lamellar ABC melts is the trilayer **ABC** with the layers **A**, **B**, and **C** formed by incompatible monomers A , B and C , respectively, and we assume no overlap between the layers. The incompressibility conditions read

$$\sigma_{\text{tri}} h_i = n_i v_0, \quad i = A, B, C \quad (2.13)$$

where $\sigma_{\text{tri}} = S_{\text{tri}}/M_{\text{tri}}$ is the surface area per one chain (S_{tri} and M_{tri} being the total area of the **AC** interfaces in all trilayers and the total number of the triblock copolymer chains in the system, respectively), n_i is the number of monomers per block of the sort i , and h_i is the width of the layer filled by such blocks. In the reduced variables the conditions 2.13 take the form

$$\Sigma_{\text{tri}} H_i = n_i, \quad i = A, B, C \quad (2.13a)$$

where $\Sigma_{\text{tri}} = \sigma_{\text{tri}} l/v_0$ is the reduced area per triblock copolymer chain and $H_i = h_i/l$ is the reduced width of the layer filled by the monomers of the i th sort.

Now, the specific (per chain) free energy of a lamellar trilayer **ABC** structure reads

$$f_{\text{tri}} = \sigma_{\text{tri}} \gamma_{\text{tri}} + f_{\text{tri}}^{\text{el}} + \sum_{i=A,B,C} n_i f_i, \quad (2.14)$$

$$\gamma_{\text{tri}} = \gamma_{AB} + \gamma_{BC}$$

Here γ_{AB} and γ_{BC} are the interfacial tensions for the interface **AB** and **BC**, respectively, and

$$f_{\text{tri}}^{\text{el}} = \frac{3T}{2} \left(\frac{H_A^2}{n_A} + \frac{H_B^2}{n_B} + \frac{H_C^2}{n_C} \right) = \frac{3T N_{\text{tri}}}{2 \Sigma_{\text{tri}}^2} \quad (2.15)$$

is the elastic (stretching) free energy per triblock copolymer chain, $N_{\text{tri}} = n_A + n_B + n_C$ being the total degree of polymerization of triblock copolymer. Given the value of the reduced surface per chain Σ_{tri} , the total free energy of the system would read

$$F_{\text{tri}} = T M_{\text{tri}} \left(\tilde{\gamma}_{\text{tri}} \Sigma_{\text{tri}} + \frac{3 N_{\text{tri}}}{2 \Sigma_{\text{tri}}^2} \right) + M_{\text{tri}} N_{\text{tri}} \sum_{i=A,B,C} x_i f_i \quad (2.16)$$

where $x_i = h_i/(h_A + h_B + h_C) = n_i/N_{\text{tri}}$ ($i = A, B, C$), and $\tilde{\gamma}_{\text{tri}} = (\gamma_{\text{tri}} \nu_0)/(lT)$ is the reduced interfacial free energy. Similar to eqs 2.4, 2.5, the rhs of eq 2.16 is still to be minimized with respect to Σ_{tri} , which gives

$$\Sigma_{\text{tri}}^{\text{eq}} = (3 N_{\text{tri}} / \tilde{\gamma}_{\text{tri}})^{1/3},$$

$$f_{\text{tri}}^{\text{eq}} = (3T/2) (3 \tilde{\gamma}_{\text{tri}}^2 N_{\text{tri}})^{1/3} + N_{\text{tri}} \sum_{i=A,B,C} x_i f_i \quad (2.17)$$

Within the approximations 2.8, 2.9, and 2.11 the effective specific surface energy $\tilde{\gamma}_{\text{tri}}$ and the free energy of forming the **ABC** lamellar structure from a homogeneous melt per chain read

$$\tilde{\gamma}_{\text{tri}} = \left((\chi_{AB}/6)^{1/2} + (\chi_{BC}/6)^{1/2} \right)$$

$$= (\chi_{AC}/6)^{1/2} (|1+y| + |1-y|)/2 \quad (2.18)$$

$$\Delta f_{\text{tri}}^{\text{lam}}/T = \left[f_{\text{tri}}^{\text{eq}} - N_{\text{tri}} \nu_0 f(x_A, x_B, x_C) \right] / T$$

$$= (3/4) (|1+y| + |1-y|)^{2/3} \tilde{\chi}^{1/3}$$

$$- \tilde{\chi} (x_A x_C + x_B ((1+y)^2 x_A + (1-y)^2 x_C) / 4) \quad (2.19)$$

where now $\tilde{\chi} = \chi_{AC} N_{\text{tri}}$ and $y = (2\delta_B - \delta_A - \delta_C)/(\delta_A - \delta_C)$ is the selectivity parameter.²⁴

As seen from 2.19, $\Delta f_{\text{tri}}^{\text{lam}}$ is negative and, thus, the lamellar phase of the symmetric ternary **ABC** triblock copolymer ($x_A = x_C = (1 - x_B)/2$) with three well-defined layers **A**, **B** and **C** is thermodynamically advantageous as compared to the disordered one for

$$\tilde{\chi} \geq \tilde{\chi}_{\text{tr}} = \frac{3\sqrt{3}(|1+y| + |1-y|)}{(1-x_B)^{3/2}(1+y^2 x_B)^{3/2}} \quad (2.20)$$

It is worthwhile to give some comments here. First, the phases with mixed layers (e.g., **A** and **BC** etc.) are, in general, also possible,¹⁷ but for simplicity we neglect this option in the present

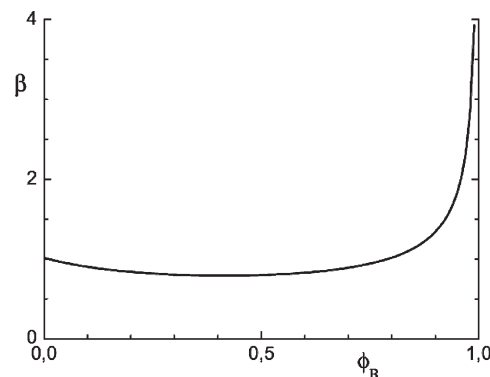


Figure 2. Comparison of the AdG and random phase approximations for the melts of the symmetric linear ternary **ABC** block copolymers with the nonselective middle block (see explanation in the text).

paper, which makes sense if all three interfacial energies γ_{AB} , γ_{AC} , γ_{BC} are large enough. Second, it follows from eq 2.20 that the x_B -dependence of $\tilde{\chi}_{\text{tr}}$ for the symmetric **ABC** linear block copolymer with $y = 0$ (nonselective middle block) reads

$$\tilde{\chi} \geq \tilde{\chi}_{\text{tr}}^{\text{AG}} = 6\sqrt{3}/(1-x_B)^{3/2} \quad (2.21)$$

Remarkably, the strict calculations based on the multicomponent random phase approximation^{14,24} show that the ratio $\beta(x_B) = \tilde{\chi}_{\text{tr}}^{\text{RPA}}(x_B)/\tilde{\chi}_{\text{tr}}^{\text{AG}}(x_B)$ differs numerically from unity by no more than 20% within the interval $0 \leq x_B \leq 0.87$ (see Figure 2). For $x_B > 0.87$, this ratio increases but it does not exceed a value of 4 even at $x_B = 0.99$, which is far beyond the AdG approximation applicability region.

Again, taking into account the scaling nature of the AdG approximation,²³ the discrepancy described should be considered as a rather minor one. This fact supports using the AdG approximation as a reasonable estimate of the free energy of NCL morphology in what follows.

2.3. Blends of Di- and Triblock Copolymers. Hereafter in this paper, we consider a mixture of the **ABC** triblock and *ac* diblock copolymer chains, the corresponding total numbers of the chains being M_{tri} and M_{di} , respectively. If the **ABC** and *ac* chains are symmetric enough and incompatible enough they segregate into tri- and bilayers, **ABC** and **ac**, respectively. The total free energy of such a state is just the sum of the contributions 2.4 and 2.16 we rewrite as follows:

$$F_{23} = M_{\text{di}} \left(T \min \left(\tilde{\gamma}_{\text{di}} \Sigma_{\text{di}} + \frac{3 N_{\text{di}}}{2 \Sigma_{\text{di}}^2} \right) + N_{\text{di}} (x_A f_A + x_C f_C) \right)$$

$$+ M_{\text{tri}} \left(T \min \left(\tilde{\gamma}_{\text{tri}} \Sigma_{\text{tri}} + \frac{3 N_{\text{tri}}}{2 \Sigma_{\text{tri}}^2} \right) + N_{\text{tri}} \sum_{i=A,B,C} x_i f_i \right) \quad (2.22)$$

Minimization in 2.22 is to be done with respect to two independent variables Σ_{di} and Σ_{tri} . The final result for F_{23} reads

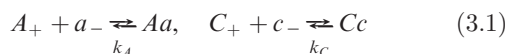
$$F_{23} = M f_{23}(r) = M \left(r f_{\text{tri}}^{\text{eq}} + (1-r) f_{\text{di}}^{\text{eq}} \right) \quad (2.23)$$

where $M = M_{\text{di}} + M_{\text{tri}}$ is the total number of macromolecules in the blend, the second equality defines the function $f_{23}(r)$, $r = M_{\text{tri}}/M$ is the number fraction of the triblock chains; the equilibrium free energies $f_{\text{di}}^{\text{eq}}$ and $f_{\text{tri}}^{\text{eq}}$ per one chain within the bilayers (trilayers) are given by eq 2.5 and eq 2.17, respectively.

It is worth to notice that the interface exchange free energies $f_A^{\text{ex}}, f_C^{\text{ex}}$ we discussed in Introduction vanish within the AdG approximation since the latter assumes that the chains belonging to different layers do not overlap at all. Thus, the sequence of the **ABC** tri- and **ac** bilayers would be random within that approximation. On the other hand, the experimental observations as well as the self-consistent Scheutjens–Fleer type calculations¹² favor the conclusion that typically both f_A^{ex} and f_C^{ex} are positive so that the blend would separate into the coexisting pure triblock and diblock lamellar phases. Since within the AdG approximation any of these options would result in the same expression 2.23 for the total free energy, in what follows we refer to both of them as the reference blend lamellar (RBL) state.

3. Centrosymmetric Pentalayer Structure in Associating Blends of Di- and Triblock Copolymers

3.1. Definitions and Pentalayer Geometry. Let a fraction α_A (α_a) of the monomers *A* (*a*) be functionalized to bear a donor (acceptor) group A_+ (a_-) and a fraction α_C (α_c) of the monomers *C* (*c*) be functionalized to bear a donor (acceptor) group C_+ (c_-), which is supposed for simplicity not to change the excluded volume of these monomers. These donor and acceptor groups are capable of forming the thermoreversible (e.g., hydrogen) bonds described, respectively, by the reactions



We assume throughout this paper that the system is in the state of chemical equilibrium as to forming and breaking the bonds which implies that the relaxation time as to achieving the thermodynamic equilibrium is small as compared to the system observation or measurement time (it is plausible until we deal with the bonds characterized by relatively small energetic barriers preventing the bond breaking). Accordingly, k_A and k_C , appearing in eq 3.1, are not the rate constants, which determine the bond formation under irreversible chemical reactions, but the temperature dependent equilibrium association constants, which determine the equilibrium distribution among various clusters of the associated chains. If the bond is well-defined and the distribution between the bonded and non-bonded states is the Gibbs one, then it is reasonable to approximate the temperature dependence of k as follows:

$$k(T) = \exp(S_{\text{bond}} - \varepsilon_{\text{bond}}/T) \quad (3.2)$$

where S_{bond} and $\varepsilon_{\text{bond}}$ are the entropy and energy of forming the bond, which are determined by its chemical nature and should be found from the experimental data or via some quantum mechanical numerical calculations. In general, the dependence $k(T)$ depends on the set of the discrete quantum states corresponding to forming the bond under consideration and could be more complicated.²⁵ In any case the numerical values of k strongly depend on the temperature.²⁶ The value of the (dimensionless) association constant determines the equilibrium number density of the bonds formed in accordance with the mass action law:^{25,27}

$$k\nu_0\nu_{\text{bond}} = k\Gamma_+\phi_+ = k\Gamma_-\phi_- = \frac{\Gamma_+\Gamma_-}{(1-\Gamma_+)(1-\Gamma_-)} \quad (3.3)$$

Here ϕ_+ and ϕ_- are the volume fractions of the donor and acceptor groups, respectively, whereas ν_{bond} and $\Gamma_{\pm} = \nu_0\nu_{\text{bond}}/\phi_{\pm}$, $\Gamma_{\pm} = \nu_0\nu_{\text{bond}}/\phi_{\pm}$ are the thermodynamically equilibrium values of the number density of bonds and so-called conversions, i.e. the fractions of the actually bonded donors and

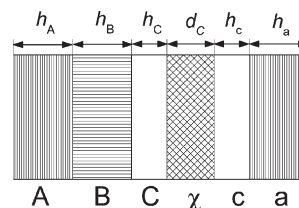


Figure 3. Elementary pentalayer geometry (see designations in the text).

acceptors. The explicit concentration and k -dependence of ν_{bond} and, thus, Γ_{\pm} can be easily found by solving eqs 3.3:

$$k\nu_0\nu_{\text{bond}} = (k\phi_+ + k\phi_- + 1 - \sqrt{(k\phi_+ + k\phi_- + 1)^2 - 4k^2\phi_+\phi_-})/2 \quad (3.4)$$

The thermoreversible association in eq 3.1 can drastically change the structure of the lamellar phase in the blends **ABC/ac**. Indeed, the association is a volume effect and, therefore, it is natural to expect (and we prove it further) that along the **Cc** (**Aa**) interfaces some layers χ (α) of a finite width d_C (d_A) may occur where the bonds Cc (Aa) between the interdigitating blocks *C* and *c* (*A* and *a*) are formed (see Figure 3).

Whereas the pure diblock (triblock) copolymer lamellar phases are built of the bi(tri)-layers **ac** (**ABC**) as the elementary “bricks”, the lamellae in the associating blends could be built of the pentalayers **ABCca** forming the centrosymmetric or noncentrosymmetric sequences **ABCcaacCBA...** (**CBAaccaABC...**) or **ABCcaABCca...**, respectively. Hereafter we refer to these structures as centrosymmetric pentalayer lamellae (CPL) and noncentrosymmetric lamellae (NCL), respectively.

To begin with, we consider thermodynamics of the pentalayer and a common layer formation assuming, for simplicity, that there is only one type of association (for definiteness, $C-c$). Then the incompressibility conditions read (in the reduced variables):

$$\Sigma_{\text{tri}}H_i = n_i, \quad i = A, B, \quad \Sigma_{\text{di}}H_a = n_a \quad (3.5a)$$

$$\Sigma_{\text{tri}}H_C = n_C - m_C^{\text{tri}}, \quad \Sigma_{\text{di}}H_c = n_c - m_C^{\text{di}} \quad (3.5b)$$

$$\Sigma_{\text{tri}}D_C\phi_C = m_C^{\text{tri}}, \quad \Sigma_{\text{di}}D_C(1 - \phi_C) = m_C^{\text{di}} \quad (3.5c)$$

Here m_C^{tri} (m_C^{di}) are the numbers of those monomers *C* (*c*) per one tri(di)block copolymer chain, which are located within the common layer, ϕ_C is the volume fraction of triblock monomers within the common layer, and $D_C = d_C/l$ is its reduced width. Now, to form the pentalayer structure the tri- and bilayers **ABC** and **ca** are to alternate. So, the total areas of the interfaces **AB** and **ca** are to be equal ($S_{\text{tri}} = S_{\text{di}} = S$) and the reduced areas Σ_{di} and Σ_{tri} are to obey the condition $\Sigma_{\text{tri}}M_{\text{tri}} = \Sigma_{\text{di}}M_{\text{di}} = \Sigma M$ or

$$\Sigma_{\text{tri}}r = \Sigma_{\text{di}}(1 - r) = \Sigma = Sl/(\nu_0M) \quad (3.6)$$

where the parameters M and r are defined in subsection 2.3 and eq 3.6 is just the definition of Σ .

3.2. Free Energy of the CPL Structure. Similar to the discussion above, the total free energy of the pentalayer **ABCca** reads

$$F_5 = F_{\text{bulk}} + \min \left\{ (T\tilde{\gamma}_{\text{di}}\Sigma_{\text{di}} + f_{\text{di}}^{\text{el}})M_{\text{di}} + (T\tilde{\gamma}_{\text{tri}}\Sigma_{\text{tri}} + f_{\text{tri}}^{\text{el}})M_{\text{tri}} \right\} + M\Sigma D_C f_{\text{d-a}}(\phi_+, \phi_-, k) \quad (3.7)$$

The first term in 3.7 describes the contribution due to the intralamellar van der Waals interaction discussed in

section 2. We assume hereafter that the fractions α_A (α_a) and α_C (α_c) of the functionalized monomers are small enough to neglect the association-due changes (if any) in the volume and self-interaction energy within the layers **A**, **B**, **C**, **χ** , **c**, and **a**, which means that no surface energy is to be assigned to the interfaces **C χ** . Besides, as consistent with the AdG approximation, we assume that segregation is complete. Thus, the total volumes of the layers depend on the lengths of the blocks only and, as such, stay the same in the pentalayer and RBL structures. Therefore, the value of F_{bulk} stays the same in all strongly segregated phases and, thus, this term can be fully disregarded when investigating the comparative stability of the pentalayer (both centro-symmetric and noncentro-symmetric) and RBL structures, and in what follows we simply omit it from all the formulas. Thus, within the AdG approximation the relative stability of the RBL and pentalayer structures is determined only by the balance of the elastic, interfacial and association contributions, which are described by two other terms in the rhs of eq 3.7.

Indeed, the second term in eq 3.7 allows for the interfacial and elastic energies. It is similar to the corresponding contribution into the free energy in eq 2.22 of the RBL state except for two important details. First, the elastic free energies per di- and triblock copolymer chains appearing in eq 3.4 differ from expressions 2.3 and 2.15 since each of the *C* and *c* blocks is now spread over two layers (**C** and **χ** , or **c** and **χ** , respectively) instead of one:

$$\begin{aligned} f_{\text{di}}^{\text{el}} &= \frac{3T}{2} \left(\frac{H_a^2}{n_a} + \frac{H_c^2}{n_c - m_C^{\text{di}}} + \frac{D_C^2}{m_C^{\text{di}}} \right) \\ &= \frac{3T}{2} \frac{N_{\text{di}}}{\Sigma_{\text{di}}^2} + \Delta f_{\text{di}}^{\text{el}}, \\ f_{\text{tri}}^{\text{el}} &= \frac{3T}{2} \left(\frac{H_A^2}{n_A} + \frac{H_B^2}{n_B} + \frac{H_C^2}{n_C - m_C^{\text{tri}}} + \frac{D_C^2}{m_C^{\text{tri}}} \right) \\ &= \frac{3T}{2} \frac{N_{\text{tri}}}{\Sigma_{\text{tri}}^2} + \Delta f_{\text{tri}}^{\text{el}} \end{aligned} \quad (3.8)$$

where the excess elastic free energies $\Delta f_{\text{tri(di)}}^{\text{el}}$ per block copolymer chain can be readily found using the incompressibility conditions:

$$\begin{aligned} \Delta f_{\text{di}}^{\text{el}} &= \frac{3T m_C^{\text{di}}}{2 \Sigma_{\text{di}}^2} \left(\frac{1}{(1 - \phi_C)^2} - 1 \right) \\ &= \frac{3T D_C}{2 \Sigma_{\text{di}}} \left(\frac{1}{1 - \phi_C} - (1 - \phi_C) \right), \\ \Delta f_{\text{tri}}^{\text{el}} &= \frac{3T m_C^{\text{tri}}}{2 \Sigma_{\text{tri}}^2} \left(\frac{1}{\phi_C^2} - 1 \right) = \frac{3T D_C}{2 \Sigma_{\text{tri}}} \left(\frac{1}{\phi_C} - \phi_C \right) \end{aligned} \quad (3.9)$$

Finally, the last contribution in 3.7 is due to thermoreversible bonding between the C_+ donors and c_- acceptors within the common **χ** layers. Here $M \Sigma d_C$ is the total volume of all common **χ** layers and $f_{\text{d-a}}$ is the specific (per unit volume) contribution to the free energy due to donor-acceptor association we discuss in more detail in the next subsection.

It follows from eqs 3.7–3.9 that the total free energy of the system reads

$$F_5 = M \min f_5(\Sigma, D_C, \phi_C) = M \bar{f}_5 \quad (3.10)$$

where the free energy f_5 per chain in the pentalayer has the form

$$f_5(\Sigma, D_C, \phi_C)/T = \bar{\gamma} \Sigma + \frac{3\bar{N}(r)}{2\Sigma^2} + D_C \Psi_C(r, \Sigma, \phi_C) \quad (3.11)$$

Here the effective degree of polymerization $\bar{N}(r) = r^3 N_{\text{tri}} + (1 - r)^3 N_{\text{di}}$ characterizes the swelling effect for pentalayers, $\gamma = \tilde{\gamma}_{\text{di}} + \tilde{\gamma}_{\text{tri}}$ is the total reduced surface tension and the function

$$T\Psi_C(r, \Sigma, \phi_C) = \Sigma f_{\text{d-a}} + \Sigma^{-1} \Delta f_{\text{el}}(r, \phi_C) \quad (3.12)$$

is the sum of the free energy gain $f_{\text{d-a}} \Sigma$ per chain due to the donor-acceptor association and the chain elastic energy change due to an extra chain stretching under their interdigitating:

$$\begin{aligned} \Delta f_{\text{el}}(r, \phi_C) &= \frac{\Sigma}{D_C} \left(\Delta f_{\text{el}}^{\text{di}}(1 - r, 1 - \phi_C) + \Delta f_{\text{el}}^{\text{tri}}(r, \phi_C) \right) \\ &= \frac{3T}{2} \left((1 - r)^2 \left(\frac{1}{1 - \phi_C} - (1 - \phi_C) \right) + r^2 \left(\frac{1}{\phi_C} - \phi_C \right) \right) \end{aligned} \quad (3.13)$$

The function $T\Psi_C$ has a simple physical meaning: it is the average per chain force causing (if $\Psi_C < 0$) or resisting to (if $\Psi_C > 0$) forming the common layer; next we call Ψ_C the interdigitating force. So, to calculate the interdigitating force and, thus, the NCL stability conditions explicitly, we are to know an explicit expression for the contribution $f_{\text{d-a}}$ into specific free energy caused by the donor-acceptor association.

3.3. Thermodynamics of Donor-Acceptor Association. The attempts to understand the nature of specific interactions (in particular, association) and to describe the thermodynamic properties of the associating systems have a long history,^{27,28} which goes beyond the scope of our paper. The most conventional approach in this field is referred to as self-associated fluid theory (SAFT)²⁸ within the physics of liquids community and the Flory approximation (see, e.g., refs 29–31 and references therein) within the polymer community.³² In particular, the contribution $f_{\text{d-a}}$ into the specific free energy per monomer caused by the donor-acceptor association within the Flory approximation reads^{38,39}

$$f_{\text{d-a}}/T = v_0 \nu_{\text{bond}} + \phi_+ \ln(1 - \Gamma_+) + \phi_- \ln(1 - \Gamma_-) \quad (3.14)$$

where ν_{bond} , Γ_+ , and Γ_- obey the mass action law in eq 3.3 and the volume fractions ϕ_+ and ϕ_- of the donor and acceptor groups, respectively, are controlled by the composition of the common layer:

$$\phi_+ = \alpha_C \phi_C, \quad \phi_- = \alpha_c (1 - \phi_C) \quad (3.15)$$

It follows from eqs 3.3, 3.4, and 3.14 that $f_{\text{d-a}} = 0$ if $k = 0$, as is expected for no association. For weak association ($k \ll 1$) one can expand the association free energy in powers of k , the first nonzero term of this expansion having the form

$$f_{\text{d-a}}/T \approx -v_0 \nu_{\text{bond}} + \dots \approx -k \phi_+ \phi_- \quad (3.14a)$$

If one considers eq 3.14a as an exact one, one arrives to an approximation, in which the association (specific interactions) results only in decrease of the effective Flory–Huggins parameter χ proportional to the association constant (see, e.g., ref 40 where the association constant k has been also

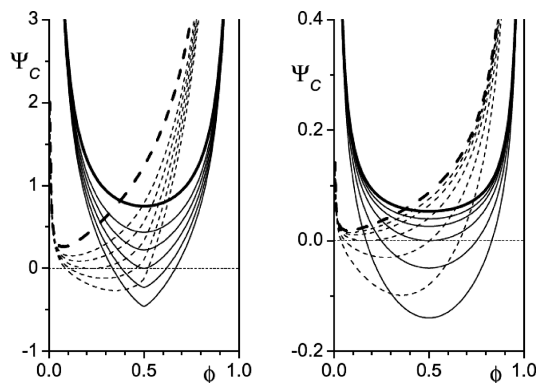


Figure 4. Typical behavior of the interdigitating force $\Psi_C(\phi)$ for various values of the association constant k (for definiteness, $n_i = 100$, $i = a, c, A, B, C$; $\chi N_{di} = \tilde{\chi} = 25$; $y = 0$; $\alpha_C = \alpha_c = 0.2$) for high stretching $\Sigma = 1$ (left) and low stretching $\Sigma = N_{di}^{1/2}$ (right). The solid and dashed lines correspond to the symmetric ($r = 0.5$) and asymmetric ($r = 0.1$) compositions, $\Psi_C < 0$ favors the common layer formation. The upper bold lines correspond to no association ($k = 0$), the thin lines do to increasing values of the association constant k and shift down monotonously with increase of k . Key: left, $k = 10^{n-3}k_0$, $n = 1-5$, where $k_0 = 47750$ for symmetric ($r = 0.5$) and $k_0 = 206720$ for asymmetric ($r = 0.1$) blends; right, $k = 2^{n-3}k_0$, $n = 1-5$, where $k_0 = 0.38924$ for symmetric ($r = 0.5$) and $k_0 = 0.32981$ for asymmetric ($r = 0.1$) blends.

evaluated). E.g., approximation 3.14a has been used to study microphase separation in associating systems within the weak segregation approach.⁴¹ Comparing eqs 3.14 and 3.14a, we see that for strong association ($k \gg 1$) approximation 3.14a considerably overestimates the association effects.

3.4. The Interdigitating Force. Combining eqs 3.12–3.15 we can now build the typical plots, which demonstrate the dependence of the interdigitating force Ψ_C on the composition $\phi = \phi_C$ in the common layer for various values of the equilibrium association constant k and triblock composition r in the bulk. The plots are presented in Figure 4 for various stretching of the blocks to be drawn into the common layer. For simplicity the degrees of polymerization of both C and c blocks are taken to be equal: $n_C = n_c = N_{di}/2$. The degree of stretching is characterized by the value of Σ . Indeed, it follows from eq 2.1a that the value of Σ for the stretched blocks is to be restricted to the interval $1 \leq \Sigma^2 \leq N_{di}$, where the left and right limits correspond to the fully stretched chain ($h \sim N_{di}l$) and the Gaussian coil $h^2 = N_{di}l^2$, respectively.

As seen from eqs 3.12 and 3.13 and Figure 4, the interdigitating force is always positive when no association is present ($k = 0$), the common layer being mostly unfavorable at the mostly asymmetric compositions within the common layer ($\phi \rightarrow 0$ and $\phi \rightarrow 1$). With increase of the association constant k the minimum of the interdigitating force $\bar{\Psi}_C(k) = \min \Psi_C(\phi)$ decreases and Ψ_C changes its sign at certain threshold value $k = k_0$. It means that for $k > k_0$ the common layers become thermodynamically favorable if their composition lies within an intermediate interval (ϕ_1, ϕ_2) where $\Psi(\phi_i) = 0$. The common layer for $\Sigma = 1$ (the stretched blocks) becomes stable for much higher values of k than that for $\Sigma = N^{1/2}$ (the coiled blocks). The reason for that is quite clear: when the common layer occurs, it involves an additional stretching of the blocks and to stretch further the blocks which have been already strongly stretched is much more expensive in terms of elastic entropy as compared to the nonstretched blocks.

In conclusion of this subsection we make two more remarks. First, the cusp, which seems to appear in curves $\Psi(\phi)$ for high stretching with increase of the value of the association constant k , is only an apparent one. In fact, the curves

are continuous but reveal a sharp crossover between the regimes with $k|\phi_+ - \phi_-| \ll \phi_+ + \phi_-$ and $k|\phi_+ - \phi_-| \gg \phi_+ + \phi_-$ since in the latter regime eq 3.4 is approximated as

$$v_0 v_{\text{bond}} = \min(\phi_+, \phi_-) \quad (3.4a)$$

which is discontinuous at $\phi_+ = \phi_-$ ($\phi = 1/2$ in our case). Equation 3.4a has a simple physical meaning: all available donors and acceptors form bonds if $k \gg 1$. Second, comparing our model calculations with the real experimental data²⁶ we see that formation of the common layer χ is a rather realistic situation.

3.5. Minimization of the CPL Free Energy. The threshold $k = k_0(r, \Sigma)$ we just discussed characterizes occurrence of the CPL phase at a specified composition r , and its calculation does not provide the full understanding of the CPL phase stability in the whole range of composition $0 \leq r \leq 1$ yet. We start the desired full analysis by reminding that, as discussed in subsection 3.2, we are to omit the volume energetic term F_{bulk} from all the expressions for the free energy. It reduces the expressions 2.5, 2.17, and 2.23 for the free energy of the RBL phase and expression 3.11 for the CPL phase to the following form:

$$f_{23}(r)/T = (3/2) \left(r \left(3\tilde{\gamma}_3^2 N_{\text{tri}} \right)^{1/3} + (1-r) \left(3\tilde{\gamma}_2^2 N_{\text{di}} \right)^{1/3} \right) \quad (2.23a)$$

$$\bar{f}_5(r, k)/T = \min \left(\bar{\gamma}\Sigma + \frac{3\bar{N}(r)}{2\Sigma^2} + D_C \Psi_C(r, \Sigma, \phi_C) \right) \quad (3.11a)$$

where the minimum implied in eq 3.11a is to be sought with respect to (i) the reduced area per chain Σ , (ii) the reduced width of the common layer D_C , and (iii) the volume fraction ϕ_C of those C monomers, which belong to the triblock chains given the number fraction r of the triblock copolymers in the blend.

To begin with, we minimize the interdigitating force $\Psi_C(r, \Sigma, \phi_C)$ appearing in the rhs of eq 3.11a with respect to the volume fraction ϕ_C of the triblock copolymer monomers within the common layer, given the values of r and Σ . As seen in Figure 4, there is a minimum of the interdigitating force $\Psi_C(r, \Sigma, \phi_C)$ with respect to ϕ_C . The corresponding minimum condition $(\partial \Psi_C / \partial \phi_C)_{r, \Sigma} = 0$ reads

$$\partial \Delta f_{\text{el}}(r, \phi_C) / \partial \phi_C = -\Sigma^2 \partial f_{\text{d-a}}(\alpha_C \phi_C, \alpha_c(1 - \phi_C), k) / \partial \phi_C \quad (3.16)$$

The location $\phi_C^{\text{eq}}(\Sigma, r)$ and value $\bar{\Psi}_C(r, \Sigma)$ of this minimum are some functions of Σ and r .

Now, since the function to be minimized in the rhs of 3.11a is linear with respect to D_C , the minimum over D_C can be located only at one of the ends of the interval of its possible values:

$$D_C = \begin{cases} 0, & \bar{\Psi}_C > 0 \\ D_C^{\text{max}}, & \bar{\Psi}_C < 0 \end{cases} \quad (3.17)$$

To find the value of D_C^{max} we notice that increase of the common layer's volume is due to drawing of the $m_C^{\text{di}}, m_C^{\text{tri}}$ monomers of both blocks into the common χ layer. Thus, if the volume fraction ϕ_C of the triblock copolymer monomers within the common layer is fixed, the increase of D_C ends as soon as at least one of the C blocks is fully sucked into the common layer. This consideration in common with the

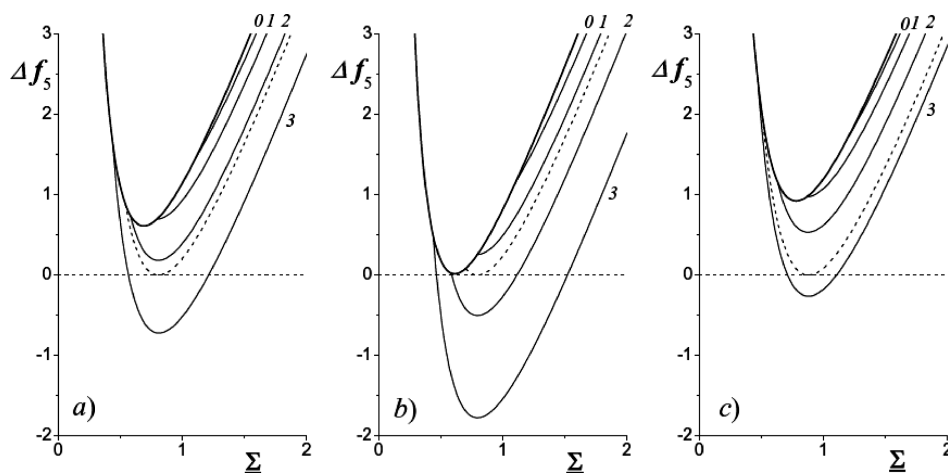


Figure 5. Typical dependences of the shifted pentalayer free energy per chain $\Delta f_5 = f_5(\Sigma, r) - f_{23}(r)$ of $\Sigma = \Sigma/N_{di}^{1/2}$ for the same system as in Figure 4 for $r = 0.25$ (a), $r = r_0 = 0.4804$ (b), and $r = 0.75$ (c) and different values of the association constant k . The upper (bold) line corresponds to no association ($k = 0$); the thin solid line labeled by the integer n and the dashed line correspond to $k = 2^{n-1}k_1(r)$ and $k = k_2(r)$, respectively, where the parameters k_1 and k_2 are defined in the text. For this particular system k_1 and k_2 are equal to 0.9132 and 2.1692 (a), 0.9678 and 1.2803 (b), and 0.7588 and 2.5037 (c), respectively. The quantity r_0 is defined by eq 3.26.

incompressibility conditions in eqs 3.5c and eq 3.6 results in the following expression for D_C^{\max} :

$$D_C^{\max}(r, \phi_C) = \frac{rn_C + (1-r)n_c}{\Sigma} \min\left(\frac{\bar{\phi}_C}{\phi_C}, \frac{1-\bar{\phi}_C}{1-\phi_C}\right) \quad (3.18)$$

where $\bar{\phi}_C = rn_C/(rn_C + (1-r)n_c)$.

The meaning of eq 3.18 is rather clear: if $k > k_0$ and the equilibrium value of ϕ_C is bigger than that averaged over the whole **C** χ **c** layer value $\bar{\phi}_C$, then the whole block **C** and a part of block **c** are sucked into the common layer whereas the rest of monomers **C** belonging to the diblocks form a pure **c** layer. Vice versa, if $\phi_C < \bar{\phi}_C$ the whole block **c** and a part of block **C** are sucked into the common layer whereas the rest of monomers **C** belonging to the triblocks form a pure **C** layer. It is worth to stress that the complete threshold “sucking” of either the **C** or **c** block into the overlap region is a rigorous consequence of our consideration based on the AdG model. However, we do not exclude that the effect could be somewhat smoother within a more accurate approximation (e.g., SCFT).

It follows from eq 3.16 and definition 3.12 that $\Psi_C(r, \Sigma, \phi_C) > 0$ for $\Sigma < \Sigma_C^{\text{lim}}$ and $\Psi_C(r, \Sigma, \phi_C) < 0$ for $\Sigma > \Sigma_C^{\text{lim}}$. To put it in other words, interdigitating becomes favorable only for stretching below certain threshold value, which is characterized by the value $\Sigma = \Sigma_C^{\text{lim}}$ where the threshold $\Sigma_C^{\text{lim}} = \Sigma_C^{\text{lim}}(r, x_C, x_c, k)$ is determined by two simultaneous equations:

$$\begin{aligned} (\partial\Psi_C(r, \Sigma, \phi_C)/\partial\phi_C)_{r, \Sigma_C^{\text{lim}}} &= 0, \\ \Psi_C(r, \Sigma_C^{\text{lim}}, \phi_C) &= 0 \end{aligned} \quad (3.19)$$

Thus, the free energy of the CPL structure can be written as the function of Σ , k and r only:

$$\begin{aligned} \bar{f}_5(r, k) &= \min_{\Sigma} f_5(r, \Sigma, k) = T \times \\ &\min \left[\bar{\gamma}\Sigma + \frac{3\bar{N}(r)}{2\Sigma^2} + \Theta(\Sigma - \Sigma_C^{\text{lim}}(k, r))\Delta f_C(r, \Sigma) \right] \end{aligned} \quad (3.11b)$$

where the Heaviside step function $\Theta(x)$ ($\Theta = 0$ if $x < 0$, $\Theta = 1$ if $x > 0$) allows for the fact that for $\Sigma < \Sigma_C^{\text{lim}}$ the common

layer χ does not exist even as a metastable one and

$$\Delta f_C(r, \Sigma) = \min\{D_C^{\max}(r, \phi_C)\Psi_C(r, \Sigma, \phi_C)\} \quad (3.20)$$

In eqs 3.11b and 3.20, the minimum is to be sought with respect to Σ and ϕ_C , respectively. The typical Σ -dependences of $f_5(\Sigma)$ are presented for different values of k in Figure 5.

As seen from Figure 5, there are two important threshold values of k . For $k < k_1$, where k_1 is determined by equation

$$\partial f_5(\Sigma, k)/\partial \Sigma|_{\Sigma=\Sigma_C^{\text{lim}}+0} = 0 \quad (3.21)$$

$f_5(r, \Sigma, k)$ as a function of Σ has a single k -independent minimum at $\Sigma = \Sigma_5^0 = (3\bar{N}(r)/(2\bar{\gamma}))^{1/3}$, which corresponds to the pentalayer structure without a common layer. Regardless of whether such a structure is really stable (actually, it is not) its free energy is a useful reference function we formally define as the value of this minimum and refer to as $\bar{f}_5^0(r)$:

$$\begin{aligned} \bar{f}_5^0(r) &= \min f_5(r, \Sigma, k)|_{d_C=0} = (3/2)T\bar{\gamma}\Sigma_5^0 \\ &= (3/2)^{4/3}T(\bar{\gamma}^2\bar{N}(r))^{1/3} \end{aligned} \quad (3.22)$$

For $k > k_1$ the function $f_5(r, \Sigma, k)$ acquires a minimum at $\Sigma = \Sigma_{\text{CPL}}(r, k) > \Sigma_5^0(r)$ corresponding to a pentalayer lamellar structure *with* a common layer (i.e., to the CPL structure). The equality $\Sigma_{\text{CPL}}(r, k) > \Sigma_5^0(r)$ means that formation of a common layer always results in a sort of relative “squeezing” the chains in lamellae (see eqs 3.5 and 3.6). We refer to the corresponding minimal value of the free energy as the CPL free energy:

$$\bar{f}_{\text{CPL}}(r, k) = \min f_5(r, \Sigma, k) = f_5(r, \Sigma_{\text{CPL}}, k) \quad (3.23)$$

Another important threshold value of the association constant k is k_2 determined by condition

$$\bar{f}_C^{\text{ex}}(r, k_2) = 0 \quad (3.24)$$

where

$$\bar{f}_C^{\text{ex}}(r, k) = \bar{f}_{\text{CPL}}(r, k) - f_{23}(r) \quad (3.25)$$

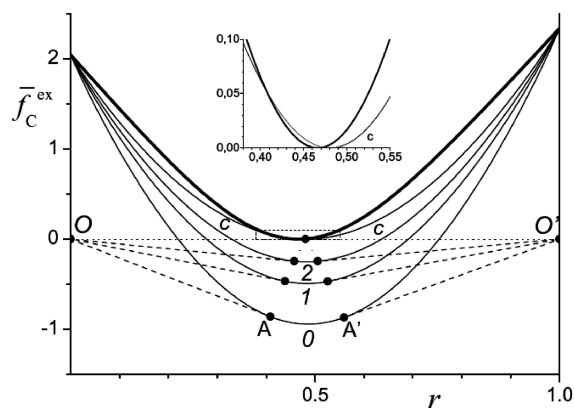


Figure 6. The typical composition dependences of the exchange pentalayer free energy 3.25 for the same system as in Figures 4 and 5. The bold line corresponds to the pentalayer structure *without* a common layer ($k = 0$), the thin solid lines labeled by integers n and the letter c correspond to the CPL with $k = k_0(1 + 2^{-n})$ and $k = k_0 = 1.2756$ and ($n = \infty$), respectively. The horizontal straight line OO' corresponds to the RBL state, the dashed lines OA and $O'A'$ are described in the text, the nodes indicate the free energies and compositions of the CPL phase coexisting with a pure di- or triblock copolymer phase (they correspond to mixture compositions defined as \bar{r}_1, \bar{r}_2 in the main text). The enhanced region within the dashed rectangular is shown in the onset.

is just the specific (per chain) dimensionless exchange free energy for the C and c layers we discussed in the Introduction. Obviously, the system under consideration forms the CPL rather than the RBL phase if $\bar{f}_C^{\text{ex}}(r, k) < 0$ and *vice versa* if $\bar{f}_C^{\text{ex}}(r, k) > 0$. Both threshold values k_1 and k_2 are the functions of the ABC/AC blend composition r , reduced surface tensions etc.

It is also worth to notice that the right parts of the plots in Figure 5 (for $\Sigma = \Sigma/N^{1/2} > 1$) have an heuristic significance only. Indeed, here the blocks are shrunk and expressions 2.3, 2.15, and 3.8 etc. for the elastic free energies are to be appended by a term describing entropy of squeezing the corresponding block into a narrow lamella, which is not expected to change our results qualitatively.

Summarizing, given the composition r , (i) the CPL structure is stable if $k > k_2(r)$, (ii) it is stable with respect to small changes of the lamella width but metastable with respect to the CPL decomposition into the RBL phase of the same average composition if $k_1(r) < k < k_2(r)$, and (iii) the CPL is absolutely unstable with respect to stretching the lamellae followed by total collapse of the common layer if $k < k_1(r)$.

3.6. Phase Equilibrium. To complete our study of the conditions for the CPL to exist we consider now the stability of the blend ABC/ac with respect to separation into macroscopic phases of different composition. Indeed, the association-induced formation of a common Cc layer and the resulting increase of stability of the CPL structure change drastically the phase equilibrium in the system. To demonstrate it we present in Figure 6 the plots of the exchange free energy defined by eq 3.25 for different values of k .

First, the auxiliary free energy $\bar{f}_5^0(r)$ for the pentalayer structure *without* a common layer (the bold line in Figure 6), which is defined by eq 3.22, exceeds that of the RBL phase within the whole interval of compositions $0 \leq r \leq 1$ but one point

$$r = r_0 = \Sigma_{\text{di}}^{\text{eq}} / (\Sigma_{\text{di}}^{\text{eq}} + \Sigma_{\text{tri}}^{\text{eq}}) \quad (3.26)$$

where $\Sigma_{\text{di}}^{\text{eq}}$ and $\Sigma_{\text{tri}}^{\text{eq}}$ are the equilibrium specific areas for pure components defined in eqs 2.5 and 2.17. Physically it means

that for this (and only for this) specific value of composition r the specific areas of pure bi- and trilayers are so tuned that they could be combined into pentlayers without any thermodynamic loss. (It can be done just by permutations of the layers without any change of their internal structure since the corresponding entropy is zero in our approximation.)

On the contrary, if the association is strong enough then the free energy of the CPL *with* a common layer (the thin lines 0, 1, 2 in Figure 6) becomes lower than the RBL state free energy. More precisely, for $k > k_t^{\text{CPL}}(\tilde{\chi}, N_{\text{di}}, x_B)$ there is a composition interval $r_1(k) < r < r_2(k)$ where $\bar{f}_C^{\text{ex}}(r, k) < 0$ and, thus, the CPL phase is more thermodynamically advantageous than the RBL state of the same composition. As is shown in Figure 6, at $k = k_t^{\text{CPL}}$, when the free energy curve $\bar{f}_C^{\text{ex}}(r)$ first touches the r -axis, $r_1 = r_2 = r_t$. The width of the interval $r_2 - r_1$ increases with increase of k .

Now, let us take into account possible phase separation into coexisting phases of different average composition. It can be checked easily⁴² that, in fact, the CPL phase is equilibrium only for compositions within an interval $\bar{r}_1(k) < r < \bar{r}_2(k)$, where the compositions $\bar{r}_1(k)$ and $\bar{r}_2(k)$ are determined (see Figure 6) by plotting the tangents OA and $O'A'$ to the exchange free energy curve $\bar{f}_C^{\text{ex}}(r)$ from the point $r = 0, \bar{f}_C^{\text{ex}} = 0$ and $r = 1, \bar{f}_C^{\text{ex}} = 0$, respectively (therewith $r_1(k) < \bar{r}_1(k) < \bar{r}_2(k) < r_2(k)$). Outside this interval the equilibrium blend under consideration separates into two phases: (i) the pure diblock copolymer lamellar phase and the CPL with $r_{\text{CPL}} = \bar{r}_1(k)$ for $0 < r < \bar{r}_1(k)$; (ii) the pure triblock copolymer phase and the CPL with $r_{\text{CPL}} = \bar{r}_2(k)$ for $\bar{r}_2(k) < r < 1$.

A diagram demonstrating a typical change of the state of the phase equilibrium in the blend studied with increase of k at a fixed value of $\tilde{\chi}$ is shown in Figure 7. It is seen that for $k < k_t^{\text{CPL}}$ the blend stays in the RBL state, whereas for $k > k_t^{\text{CPL}}$ the blend could stay either in one of two phase-separated states (AC+CPL and ABC+CPL) or in one-phase CPL state. Thus, the point $k = k_t^{\text{CPL}}, r = r_t$ is the triple point for the system under consideration.

It is worth to notice that the diagram shown in Figure 7 is a sort of *demo* diagram rather than the genuine phase diagram since in a real system both the association constant k and the incompatibility parameter $\tilde{\chi}$ depend on the temperature and, thus, are changing simultaneously. The examples of the genuine phase diagrams will be presented in section 5.

4. NCL in Associating Blends of Di- and Triblock Copolymers

4.1. The Free Energy of the NCL Structure. The preceding analysis of the CPL structure in associating ABC/ac blends can be easily generalized to the case when both association constants k_A and k_C are finite. Then both exchange free energies could become negative, which would result in formation of the NCL structure $CBAacCBAac...$. The only difference is that now there are two associating layers instead of one: the χ layer of mixed c and C blocks and α layer of mixed a and A blocks. Accordingly, apart from the incompressibility conditions 3.2 one more condition for the common layer α holds:

$$\Sigma_{\text{tri}} D_A \phi_A = m_A^{\text{tri}}, \quad \Sigma_{\text{di}} D_A (1 - \phi_A) = m_A^{\text{di}} \quad (4.1)$$

Here $m_A^{\text{tri}}(m_A^{\text{di}})$ are the numbers of those monomers A (a) belonging to the tri- and diblock copolymers, respectively, which are located within the common layer α , ϕ_A is the volume fraction of A monomers in the layer, and $D_A = d_A/a$ is its reduced width. Applying the preceding consideration of the common layer χ to the α layer, one gets readily the NCL

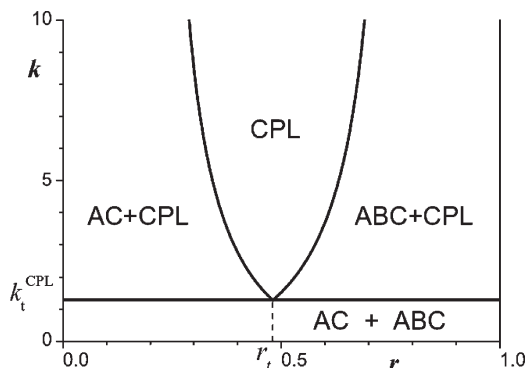


Figure 7. A *demo* diagram in the plane (r, k) demonstrating the phase equilibrium in the same system as in Figures 4–6. The vertical dashed line is the guide for eyes indicating the location of the triple point ($r_t = 0.4804$, $k_t^{\text{CPL}} = 1.2756$).

free energy per chain:

$$F_{\text{NCL}}(r) = M \min f_{\text{NCL}}(r, \Sigma, k_A, k_C) \quad (4.2)$$

$$\begin{aligned} f_{\text{NCL}}(r, \Sigma, k_A, k_C)/T = & \bar{\gamma}\Sigma + \frac{\bar{N}(r)}{2\Sigma^2} + \Theta(\Sigma - \Sigma_C^{\text{lim}}(k_C, r))\Delta f_C \\ & + \Theta(\Sigma - \Sigma_A^{\text{lim}}(k_A, r))\Delta f_A \end{aligned} \quad (4.3)$$

where $\Sigma_C^{\text{lim}}(k_C, r)$, $\Delta f_C(r, \Sigma)$ are defined by eqs 3.19 and 3.20, respectively, whereas $\Sigma_A^{\text{lim}}(k_A, r)$ and $\Delta f_A(r, \Sigma)$ are defined by the equalities identical to eqs 3.19, 3.20 but replacing the indices C with A .

4.2. The Triple Point and Its Dependence on the System Architecture. Complete analysis of the free energy 4.2–4.3 as a function of both association constants k_A and k_C as well as the architecture parameters n_i , α_j and the parameters of volume interactions χ_{AB} , χ_{BC} , and χ_{AC} is a mostly straightforward but rather cumbersome task. To avoid an over-amplification of this paper we omit such a complete analysis here (we hope to provide it elsewhere). Instead, to give the reader a general idea of the physical effect of the NCL structure formation, we consider in this paper the blends of completely symmetric di- and triblock copolymers only. Namely, we set

$$\begin{aligned} n_a &= n_c = n_A = n_C = n; \\ n_B &= 2nx_B/(1-x_B); \quad \chi_{AC} = 4\chi_{AB} = 4\chi_{BC} = \chi; \\ k_A &= k_C = k; \quad \alpha_A = \alpha_C = \alpha_a = \alpha_c = \alpha \end{aligned} \quad (4.4)$$

Thus, the lengths of the side blocks A, C (a, c) are characterized by the single length n . The middle block is assumed to be nonselective ($y = 0$). Finally, both the degrees of functionalization of the side blocks and the association constants are assumed to be equal (as if one uses the same donor (acceptor) groups to functionalize both A and C (a and c , respectively) blocks).

In such a symmetric case, eq 4.3 is simplified radically and reads

$$f_{\text{NCL}}(r, \Sigma, k)/T = \bar{\gamma}\Sigma + \frac{\bar{N}(r)}{2\Sigma^2} + 2\Theta(\Sigma - \Sigma^{\text{lim}}(k, r))\Delta f_C \quad (4.5)$$

which differs from the pentalayer free energy in eq 3.11a only by appearance of the additional factor of 2 before the Θ -function to allow for two (rather than one as in the previous

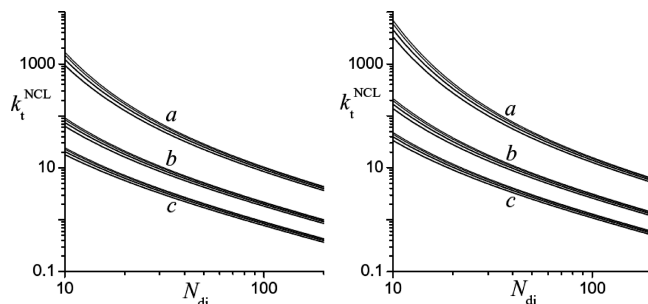


Figure 8. The triple point k_t^{NCL} value of the thermoreversible association constant k as a function of the total diblock copolymer degree of polymerization N_{di} for $\tilde{\chi} = \chi N_{\text{di}} = 20$ (left) and $\tilde{\chi} = 50$ (right) and various architecture parameters. The labels a , b and c correspond to the blends with degrees of functionalization α equal to 0.1, 0.2 and 0.3, respectively; therewith for each value of α we present four curves, which correspond (from the top to the bottom in each family of curves) to $x_B = 1/3, 1/2, 2/3$ and $4/5$, respectively.

section) common layers. So, the behavior of the free energy in eq 4.5 as a function of both Σ and r is completely similar (but some numerical factors) to that shown in Figures 5 and 6, respectively. Because of this reason and also to reduce the length of the current paper we do not present the corresponding plots here. Once again, we find easily that there is such a triple point ($k = k_t^{\text{NCL}}$, $r = r_t$) that for $k < k_t^{\text{NCL}}$ the RBL state is stable for any composition r . For $k > k_t^{\text{NCL}}$ there exists such a composition interval $\bar{r}_1(k) < r < \bar{r}_2(k)$ of the NCL phase stability that for $r < \bar{r}_1$ ($r > \bar{r}_2$) the system decomposes into the NCL phase and pure diblock (triblock) phase. The width $\bar{r}_2(k) - \bar{r}_1(k)$ of the stability interval is zero at $k = k_t^{\text{NCL}}$ where $\bar{r}_2(k) = \bar{r}_1(k) = r_t$ and increases with increase of k .

The effect of the system architecture on the triple point association constant k_t^{NCL} is demonstrated in Figure 8. As one naturally expects, the k_t^{NCL} decreases rapidly when the degree of functionalization α increases. Another important effect is that k_t^{NCL} decreases significantly with the increase of a block length n . Indeed, the interdigitating force Ψ whose sign controls the formation of the common layers is a sum of two contributions: (i) a negative one due to forming the donor-acceptor bonds, and (ii) a positive one due to the *additional elongation* of the chains. Meanwhile, the susceptibility of polymer chains to elongation is inversely proportional to the chain length (see eq 2.3 and the similar ones onward). Therefore, the increase of the chain length reduces the elastic contribution into the interdigitating force and, thus, facilitates forming the common layers. Besides, Figure 8 reveals a rather weak dependence of the k_t^{NCL} on the relative length of the middle block x_B , the existence of the dependence $k_t^{\text{NCL}}(x_B)$ is due to the fact that the chains with the longer middle block are more susceptible to elongation.

Summarizing, the results presented in this section and Figure 8 open a new root to transform the ABC/ac blends under consideration into the desired noncentrosymmetric pentalayer lamellar (NCL) morphology, which occurs in the region above the corresponding curve in Figure 8. Obviously, for this purpose, one can use (i) changing the chemistry of the functionalized groups to increase the thermoreversible association constant k , (ii) increasing the degree of polymerization n of the associating blocks $A(a)$ and $C(c)$, and (iii) increasing the degree of functionalization α of these blocks.

5. The Chemistry Effects and Global Phase Analysis

5.1. The Phase Portrait Construction. To complete the study we build here some typical phase diagrams of the symmetric associating blends ABC/ac in the plane of observable

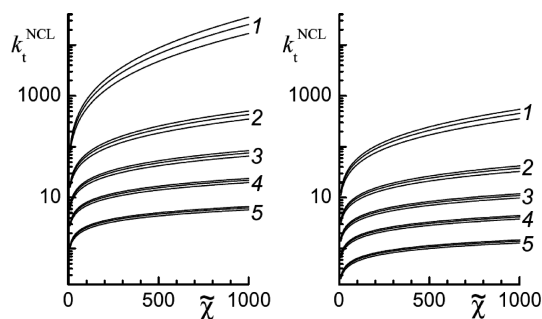


Figure 9. Triple point value k_t^{NCL} of the thermoreversible association constant k as a function of the reduced Flory parameter $\tilde{\chi}$ for the degrees of functionalization $\alpha = 0.1$ (left) and $\alpha = 0.2$ (right) and various architecture parameters. The labels 1, 2, 3, 4, and 5 correspond to the blends with $N_{\text{di}} = 20, 50, 10, 200$, and 500 , respectively; therewith for each value of α and N_{di} we present three curves, which correspond (from the top to the bottom in each family of curves) to $x_B = 1/3, 1/2$, and $2/3$, respectively.

parameters (r, T). Such phase diagrams are expected to differ from the *demo* phase diagram in the plane (r, k) presented above in Figure 7 because the association constant k is a function of the temperature T rather than an independent variable. To find all types of the phase diagrams possible in the blends under consideration we follow the method of global phase analysis also known as the global phase diagram study,^{44–47} which for the associating systems has been proposed by one of us⁴⁸ and applied in refs 49–51. The idea of this method is to split the space of the microscopic parameters of the system under consideration into regions, where the topological behavior of the phase diagrams identified by the number of their special (critical, triple etc.) points is the same, and to present typical phase diagrams for each of such regions. Thus, the global phase analysis tells whether all the systems with a specified type of microscopic interaction reveal the same universal type of the phase behavior and, if not, which changes of the microscopic interaction parameters result in a qualitative (topological) change of the system phase behavior.

Since the critical points' study is beyond the AdG approximation, in our case the only special points of the phase diagrams are the triple points. So, we start with analysis of the triple point dependence on the reduced Flory parameter. $\tilde{\chi} = \chi N_{\text{di}}$. As shown in Figure 9, the threshold value k_t^{NCL} monotonously increases with increase of $\tilde{\chi}$ and, as consistent with the results presented in Figure 8, decreases with increase of the degree of polymerization n of the associating blocks $A(a)$ and $C(c)$ and the degree of functionalization α of these blocks.

On the other hand, both the equilibrium association constant k and the Flory parameter χ depend on the temperature. We assume the simplest possible temperature dependences of these parameters:

$$\left. \begin{aligned} \chi &= \Theta/2T \\ k &= \exp(S_{\text{bond}} - \varepsilon/T) \end{aligned} \right\} \Rightarrow \ln k = S_{\text{bond}} - \tilde{E}\tilde{\chi};$$

$$\tilde{E} = 2\varepsilon/(\Theta N_{\text{di}}) = E/N_{\text{di}} \quad (5.1)$$

where S_{bond} and E are the entropy and reduced energy of the actual donor-acceptor bond, respectively. As consistent with eqs 5.1, a temperature change corresponds to a movement of the point representing the state of the system along a straight line on the $(\ln k, \tilde{\chi})$ plane. The choice of the chemical groups modifying the original $A(C)$ repeating units of the

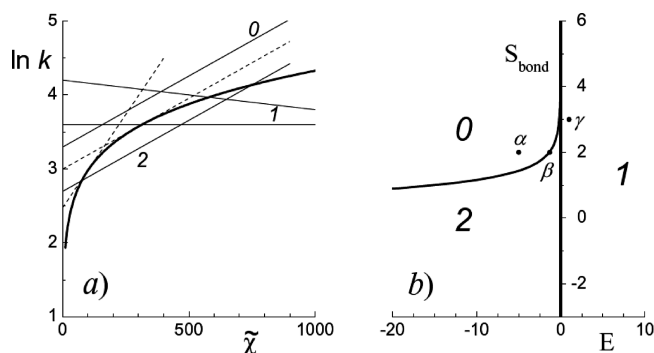


Figure 10. (a) Geometric background of the topological classification of the phase diagrams plausible in the associating block copolymer blends ABC/ac . The straight lines correspond to the actual $k(\tilde{\chi})$ dependences 5.1 with various values of the entropy and reduced energy of the donor-acceptor bond; the thin solid straight lines are labeled by the numbers of their intersections with the plot of the characteristic function $\ln k_t^{\text{NCL}}(\tilde{\chi})$ (the bold curve), the dashed straight lines are the tangents to this curve, which separate the systems with 0 and 2 triple points. (b) Typical phase portrait in the plane (reduced energy E – entropy S_{bond} of the donor-acceptor bond) for $N_{\text{di}} = 100, \alpha = 0.1$, and $x_B = 0.5$. The locus of all such tangents separating the systems with the energy and entropy of the donor-acceptor bond, which provide the phase diagrams with two and no triple points, respectively, is shown by the bold curve; the line separating the systems with the energy and entropy of the donor-acceptor bond, which provide the phase diagrams with one and even number of triple points, respectively, is $E = 0$. The dots α, β , and γ correspond to the phase diagrams shown in Figures 11, 12, and 13, respectively.

blocks $A(a)$ and $C(c)$ affects the chemical nature of the donor-acceptor bonding and, thus, results in changes in the values of S_{bond} and E . Besides, the effective values of S_{bond} and E could be controlled by adding a low-molecular concurrent inhibitor,⁴⁹ the effective entropy S_{bond} being increased when the concurrent inhibitor fugacity decreases.

Now, the triple point values of $\ln k$ and χ are determined by the requirement that the point belongs simultaneously to the curve $\ln k = \ln k_t^{\text{NCL}}(\tilde{\chi})$ and the straight line $\ln k = S_{\text{bond}} - \tilde{E}\tilde{\chi}$. In other words, the triple points are nothing but the points of intersection between these two curves. So, the number of the triple points in a specified ABC/ac blend and, therefore, its phase diagram topology, is controlled by the number of such intersections. As seen in Figure 9, the triple point curves $\ln k = \ln k_t^{\text{NCL}}(\tilde{\chi})$ have no inflection points, both the curvature and slope of the curve being approached zero in the limit $\tilde{\chi} \rightarrow \infty$. It means that, depending on the actual values of the entropy S_{bond} and reduced energy E of the donor-acceptor bond, the number of their intersections with the straight lines 5.1 could only equal 0, 1, or 2 as shown in Figure 10a, thus resulting in phase diagrams with 0, 1, or 2 triple points.

Following refs 48–51, we separate the (S_{bond}, E) -plane into the regions, which correspond to different numbers of triple points on the corresponding phase diagrams, and refer to the resulting partitioned plane (S_{bond}, E) as the “phase portrait” of the system (see Figure 10b). The main role in building such a portrait is played by the bold curve, which corresponds to the locus of the tangents to the triple point curve in Figure 10a, and separates the systems with a strong and moderate bonding. We refer to this curve as the *boundary*. We calculated the corresponding typical phase diagrams assuming for the moment that the presented consideration is valid for any positive value of $\tilde{\chi}$.

The phase behavior of the systems with **strong bonding**, whose reduced entropy and energy of the donor-acceptor bond belong to the region 0 situated above the *boundary*, is

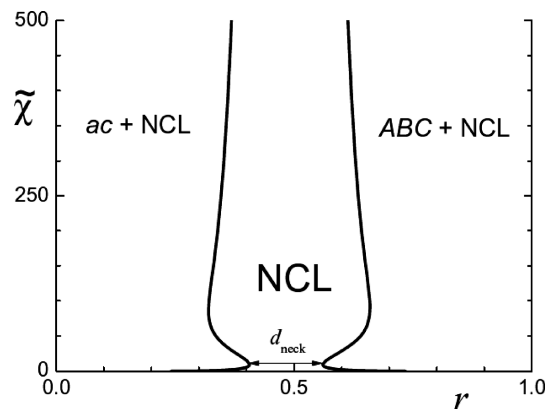


Figure 11. Typical phase diagram calculated for the system without any triple points (region 0, point α on the phase portrait shown in Figure 10b). $N_{di} = 100$, $\alpha = 0.1$, $x_B = 0.5$, $S_{bond} = 2$, and $E = -5$.

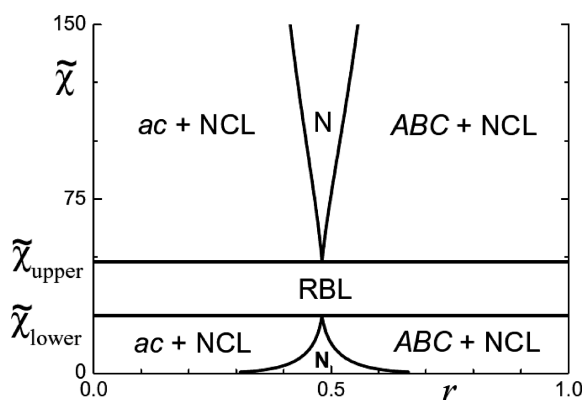


Figure 12. A typical phase diagram calculated for the system with two triple points (region 2, point β on the phase portrait shown in Figure 10b). $N_{di} = 100$, $\alpha = 0.1$, $x_B = 0.5$, $S_{bond} = 2$, and $E = -1.3$.

shown in Figure 11. In this case at any temperature (or $\tilde{\chi}$) there is an interval of concentrations delineated by two bold lines (binodals), where the only stable phase is the NCL phase. Beyond the region the melt ABC/ac separates into two coexisting phases: the pure diblock (triblock) copolymer melt left (right) to the region of NCL and the NCL phase with a temperature-dependent composition indicated by the corresponding binodal. When the representative point α in Figure 10b moves down or to right, the width d_{neck} of the neck clearly seen in Figure 11 decreases until it disappears on the boundary.

Below the boundary, i.e. for the systems with **moderate bonding**, whose reduced entropy and energy of the donor-acceptor bond belong to the region 2, the phase behavior is rather different as shown in Figure 12. To describe it properly, it is convenient to define the upper and lower triple points by analogy with the upper and lower critical solubility points. Namely, as shown in Figure 12, in this case there exists an intermediate temperature interval $T_{upper} < T < T_{lower}$ (or $\tilde{\chi}_{lower} < \tilde{\chi} < \tilde{\chi}_{upper}$) where the NCL phase could occur only as a metastable phase. Under thermodynamic equilibrium the blend is to decompose within this interval into the RBL phase, i.e. into independent bilayers ac and trilayers ABC . On the contrary, for $\tilde{\chi} > \tilde{\chi}_{upper}$ and $\tilde{\chi} < \tilde{\chi}_{lower}$, the phase behavior of the blend ABC/ac corresponds to that described in Figure 11. The definitions of the lower and upper triple points correspond to the conventional definitions of the lower and upper critical solubility points. It is worth to notice that the point β in Figure 10b, which

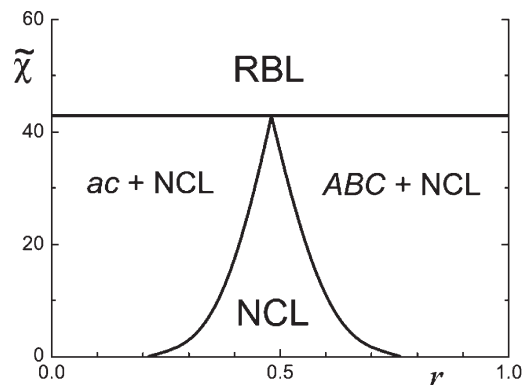


Figure 13. Typical phase diagram calculated for the system with the only triple point (region 1, point γ on the phase portrait shown in Figure 10b). $N_{di} = 100$, $\alpha = 0.1$, $x_B = 1$, $S_{bond} = 3$, and $E = 1$.

corresponds to the phase diagram shown in Figure 12, is intentionally chosen to be close to the border between the regions 0 and 2 (otherwise the value of $\tilde{\chi}_{lower}$ is typically too low). When the point β moves right, the value of $\tilde{\chi}_{upper}$ increases until $\tilde{\chi}_{upper}$ becomes infinite and, thus, the low-temperature NCL region disappears on the vertical line $E = 0$; when the point β moves down then $\tilde{\chi}_{lower}$ decreases.

Accordingly, in the right half-plane (S_{bond} , E) there is only one (high-temperature) NCL region and the only lower triple point as shown in Figure 13. We call this half-plane the region of **hydrophobic bonding** since the height $\tilde{\chi}_{lower}$ of the lower triple point (and, thus, the area of the NCL phase existence) increases with increase of the value S_{bond} of the entropy of the donor-acceptor bond. Even though the issue whether such a *hydrophobic bonding* is physically possible remains open; there are some arguments,⁴⁹ which show that such a situation could occur when some concurrent inhibitors are present in the system under consideration.

It is worth to notice two interesting features of all the phase diagrams presented in Figures 11–13. First, we find a much wider region of the NCL phase stability in the associating blends than seen previously¹³ in nonassociating ones. Second, in our case the NCL phase extends up to very high temperatures ($\chi = 0$) where it is natural to expect the system to be disordered. This apparently unphysical result is, nevertheless, correct for the values of parameters specified for the phase diagrams presented. The case is that, unlike the Flory parameters χ_{ij} , which basically approach zero when $T \rightarrow \infty$, the association constant 3.2 takes a finite value $k = \exp(-S_{bond})$ even in this limit. Therewith, the association-due gain in the free energy under concentrating the associating groups under forming a lamella of overlapping blocks A and a (C and c) exceeds the loss because of decrease in volume fraction occupied by the associating groups. Thus, surprisingly, the strongly segregated alternating lamellae of the associating A and a (C and c) blocks and Gaussian B blocks could exist even in the limit $\chi N_{di} \ll 1$. In general case the presence or absence of the high-temperature ordering would depend on particular values of S_{bond} and structure parameters of the system under consideration. In particular, for weak association when one can use approximation 3.14a, the ODT condition for symmetric blends would read $N_{di} \exp(S_{bond}) \geq 10$. We should add also that the phase transition lines corresponding to ordering in the pure components are not drawn for simplicity.

At last, the effect of the total degree of polymerization N_{di} of the symmetric associating blocks under consideration and their degree of functionalization α on the phase portraits is demonstrated in Figure 14.

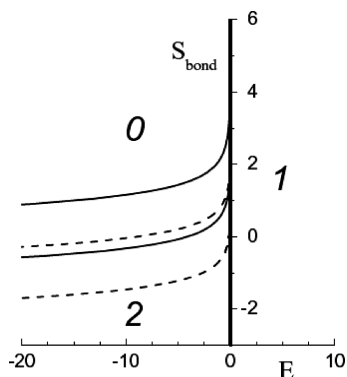


Figure 14. Phase portraits for $N_{\text{di}} = 500$, $\alpha = 0.1$, $x_B = 0.5$, and $N_{\text{di}} = 500$, $\alpha = 0.2$, $x_B = 0.5$ (the upper and lower dashed lines, respectively) and $N_{\text{di}} = 100$, $\alpha = 0.1$, $x_B = 0.5$ (the upper) and $N_{\text{di}} = 100$, $\alpha = 0.2$, $x_B = 0.5$ (the lower) solid lines, respectively.

We see that the increase of both N_{di} and α results basically in a considerable shifting the phase equilibrium in favor of the NCL phase and, accordingly, shifts the *boundary* down.

6. Discussion and Conclusions

Summarizing, in this paper we suggested a new route to create stable noncentrosymmetric lamellar morphologies in mixtures of di- and triblock-copolymers ABC/ac via a proper functionalization of the side blocks $A(C)$ of the triblock copolymer and blocks of diblock copolymer by the donor and acceptor groups. The resulting donor-acceptor association has been expected to get the a and A (c and C) blocks effectively glued together or, in other words, to reduce the exchange energies $f_{A,C}^{\text{ex}}$ introduced in ref 8 and described in the Introduction. To validate this suggestion we studied theoretically the thermodynamics of the lamellar morphologies arising in symmetric mixtures ABC/ac with the non-selective (with respect to the side blocks) middle block B with due regard for thermoreversible associating of the proper blocks. Unlike the preceding studies^{41,52–57} of microphase separation in associating block copolymer systems, which have been restricted to the weak segregation case, we addressed strongly segregated associating block copolymers via a modified Alexander–de Gennes approximation. Even though certainly less accurate than the SCFT numerical procedure, the AdG approximation is remarkably simple and less demanding in terms of computer time needed, which enabled us to explore the vast space of parameters characterizing the system under consideration. We showed that if the association constant k , which governs the donor-acceptor thermoreversible bonding, exceeds certain threshold then the expected gluing does take place and a wide region of stability of a phase with the NCL morphology arises. Therewith, depending on the values of the effective entropy and energy per bond (see definitions in eq 5.1), the phase diagrams with or without triple points are possible (see Figures 11, 12, and 13). It is worthwhile to notice that one type of our phase diagrams (that with one upper triple point) has been already found and described in the preceding SCFT study.¹³

The summary of our results is presented in Figure 14 clearly demonstrating that to favor the NCL phase stability one should increase at least one of the following factors: (i) the degree of polymerization N_{di} of the side blocks; (ii) the degree of their functionalization α ; (iii) the value of the effective entropy S and the absolute value of the negative energy E of the donor-acceptor bonding. Figure 14 provides also an idea of the quantitative magnitude of each described effect.

To conclude, let us evaluate the validity of the assumptions our consideration is based on. First, the AdG approximation,

which assumes, in particular, that the interfaces between the neighboring domains are rather sharp, is too rough to describe accurately the weak and intermediate segregation. So, it would make sense to check our predictions via a more regular procedure such as the self-consistent field theory. However, we expect, by analogy with similar calculations in the case of nonassociating systems, that such a more accurate consideration would only result in a smoothing of the interfaces but preserve the main features of the global phase behavior obtained in this paper: the presence of a well-defined crossover from the low- k regime, where no or a negligible common layer exists, to the high- k regime, where the common layer covers a significant part of the cC layer. The topological types of the phase diagrams are also expected to stay unaffected except for the regions of low values of $\tilde{\chi}$ ($\tilde{\chi} \leq 10$), where the chains within the common layers are rather shrunk than stretched, and high values of χ where the thermodynamic equilibrium is not reachable due to glassing. One should also keep in mind that the bonds are assumed to be reversible (annealed) since consideration of the frozen bonds thermodynamics would be considerably more sophisticated due to necessity to allow for the frozen heterogeneities in the spatial distribution of the frozen bonds.^{58,59} Of course, as in any theory addressing formation of structures in concentrated polymers, we disregard the relaxation effects, which could be not always true. However, we believe that our thermodynamic approach does catch the main features of the NCL structures stability in the associating block copolymer blends.

The presented approach is easily extendable to evaluate the desirable chemical modifications of other block copolymer systems^{59,60} where the noncentrosymmetric lamellar structures were observed. E.g., for the ter-block copolymers $ABCa$ one can expect formation of both centrosymmetric $ABCaaCBA...$ and noncentrosymmetric $ABCa(\alpha)ABCa...$ structures, the free energies of which obtained via a straightforward generalization of consideration in sections 3 and 4, read:

$$f_4^{\text{CL}}(\Sigma) = T \left(\bar{\gamma} \Sigma + \frac{3N_{\text{ter}}}{2\Sigma^2} \right),$$

$$f_4^{\text{NCL}}(\Sigma, D_A, \phi_C) = f_4^{\text{CL}}(\Sigma) + D_A \left(\Sigma f_{d-a} + \frac{3T}{2\Sigma} \left(\frac{1}{1-\phi_A} + \frac{1}{\phi_A} - 1 \right) \right)$$

In other words, in this case the NCL stability condition is again that the interdigitating force is negative and the corresponding analysis could be straightforwardly carried out via the approach presented in this paper. We expect the dependences of the phase transition temperature on the structure parameters to be very similar to those found here for blends and suppose to study them in more detail and compare with the SCFT results for nonassociating ter-block copolymers^{61,62} elsewhere.

Acknowledgment. We thank anonymous reviewers for valuable comments.

References and Notes

- (1) Prost, J.; de Gennes, P.-G. *The Physics of Liquid Crystals* (Clarendon Press: Oxford, U.K., 1974).
- (2) Petschek, R. G.; Wiefeling, K. M. *Phys. Rev. Lett.* **1987**, *59*, 343.
- (3) Halperin, A. *Macromolecules* **1990**, *23*, 2724.
- (4) Tournilhac, F.; Blinov, L. M.; Simon, J.; Yablonsky, S. V. *Nature* **1992**, *359*, 621.
- (5) Jacobs, A. E.; Goldner, G.; Mukamel, D. *Phys. Rev. A* **1992**, *45*, 5783.
- (6) Prost, J.; Bruinsma, R.; Tournilhac, F. *J. Phys. II Fr.* **1994**, *4*, 169.
- (7) Stupp, S. I.; LeBonheur, V.; Walker, K.; Li, L. S.; Huggins, K. E.; Keser, M.; Amstutz, A. *Science* **1997**, *276*, 384–389.

- (8) Goldacker, T.; Abetz, V.; Stadler, R.; Erukhimovich, I.; Leibler, L. *Nature* **1999**, 398, 137–139.
- (9) Abetz, V.; Goldacker, T. *Macromol. Rapid Commun.* **2000**, 21, 16.
- (10) Witten, T.; Leibler, L.; Pincus, P. A. *Macromolecules* **1990**, 23, 824.
- (11) Leibler, L.; Gay, C.; Erukhimovich, I. Ya. *Europhys. Lett.* **1999**, 46, 549.
- (12) Amoskov, V. M.; Bitshtein, T. M. *Polym. Sci., Ser. A* **2002**, 44, 954.
- (13) Wickham, R. A.; Shi, A.-C. *Macromolecules* **2001**, 34, 6487.
- (14) Erukhimovich, I. Ya. *Eur. Phys. J. E* **2005**, 18, 383.
- (15) Alexander, S. J. *Phys. (Paris)* **1977**, 38, 983.
- (16) de Gennes, P.-G. *Macromolecules* **1980**, 13, 1069.
- (17) Abetz, V.; Stadler, R.; Leibler, L. *Polym. Bull.* **1996**, 37, 135.
- (18) Birshtein, T. M.; Polotsky, A. A.; Amoskov, V. M. *Macromol. Symp.* **1999**, 146, 215.
- (19) Flory, P. J. *Principles of Polymer Chemistry*; Cornell University Press: Ithaca, NY, 1953.
- (20) Hildebrand, J. H.; Scott, R. L. *The Solubility of Nonelectrolytes*, 3rd ed.; American Chemical Society Monograph Series; American Chemical Society: Washington, DC, 1950.
- (21) Helfand, E.; Tagami, Y. *J. Chem. Phys.* **1972**, 56, 3592.
- (22) Leibler, L. *Macromolecules* **1980**, 13, 1602.
- (23) The entropic (elastic) contribution into the free energy within the AdG approximation is calculated basing on the dimensional (scaling) considerations so that the numerical factor in front of this term can not be defined precisely.
- (24) Erukhimovich, I.; Abetz, V.; Stadler, R. *Macromolecules* **1997**, 34, 7435.
- (25) Landau, L. D.; Lifshitz, E. M. *Statistical Physics*, 3rd ed., Pergamon Press: Oxford, U.K., and New York, 1980; Vol. 1.
- (26) For room temperature, the values of the dimensionless constant k for various monomers²⁷ span the range from $k \sim 1$ to $k \sim 10^{5-6}$ depending on the chemical nature of the bonds.
- (27) Coleman, M. M.; Graf, J. F.; Painter, P. C. *Specific Interactions and the Miscibility of Polymer Blends*; Technomic: Lancaster, PA, 1992.
- (28) Muller, E. A.; Gubbins, K. E. *Ind. Eng. Chem. Res.* **2001**, 40, 2193.
- (29) Erukhimovich, I. Ya. *JETP* **1995**, 81, 553.
- (30) Semenov, A. N.; Rubinstein, M. *Macromolecules* **1998**, 31, 1373.
- (31) Erukhimovich, I. Ya.; Tamm, M. V.; Ermoshkin, A. V. *Macromolecules* **2001**, 34, 5653.
- (32) Two alternative treatments (Tanaka–Stockmayer approach^{33–36} and mesoscopic cyclization approach^{29,31,37}) differ from the Flory approximation in describing the infinite labile cluster of associated particles (gel fraction). All the treatments are identical when no gel exists ($k \ll 1$), approach the Flory approximation for rather dense gel ($k \gg 1$) but result in different properties of the associating systems near the sol–gel transition ($k \sim 1$). For further discussion, which goes far beyond the scope of this paper, we address the interested reader to refs 29, 31, 36, and 37.
- (33) Tanaka, F.; Matsuyama, A. *Phys. Rev. Lett.* **1989**, 62, 2759.
- (34) Tanaka, F. *Macromolecules* **1989**, 22, 1988.
- (35) Ishida, M.; Tanaka, F. *Macromolecules* **1997**, 30, 3900.
- (36) Tanaka, F. *Phys. Rev. E* **2006**, 73, 061405.
- (37) Tamm, M. V. *The Structure of an Infinite Cluster of Labile Bonds and the Global Phase Behavior of Thermoreversibly Associating Systems*. Ph.D. Thesis, Physics Department, Moscow State University, Moscow, 2002.
- (38) Tamm, M. V.; Erukhimovich, I. Ya. *J. Chem. Phys.* **2003**, 119, 2720.
- (39) Kudryavtsev, Ya. V.; Litmanovich, A. D.; Makeev, A. G.; Bogomolov, S. V. *Macromol. Theory Simul.* **1999**, 8, 161.
- (40) ten Brinke, G.; Karasz, F. E. *Macromolecules* **1984**, 17, 815.
- (41) Cho, J.; Kwon, Y. K. *J. Polym. Sci.: Part B: Polym. Phys.* **2003**, 41, 1889.
- (42) A rigorous consideration has been presented in ref 43 for a physically different but mathematically isomorphous situation.
- (43) Erukhimovich, I. Ya.; Olvera de la Cruz, M. J. *Polym. Sci., Part B: Polym. Phys.* **2007**, 45, 3003.
- (44) Scott, R. L.; van Konynenburg, P. H. *Discuss. Faraday Soc.* **1970**, 49, 87.
- (45) Scott, R. L.; van Konynenburg, P. H. *Philos. Trans. R. Soc. London, Ser. A* **1980**, 248, 495.
- (46) Yelash, L. V.; Kraska, T. *Ber. Bunsen-Ges. Phys. Chem.* **1998**, 102, 213.
- (47) Yelash, L. V.; Kraska, T.; Deiters, U. K. *J. Chem. Phys.* **1999**, 110, 3079.
- (48) Erukhimovich, I. Ya., *Weak Supercrystallization and other Fluctuation Effects in Concentrated Flexible Polymer Systems of Complex Architecture*. D.Sc. Thesis, Moscow, 1994.
- (49) Ermoshkin, A. V.; Erukhimovich, I. Ya. *J. Chem. Phys.* **2002**, 116, 368.
- (50) Tamm, M. V.; Erukhimovich, I. Ya. *J. Chem. Phys.* **2003**, 119, 2720.
- (51) Belousov, M. V.; Tamm, M. V.; Erukhimovich, I. Ya. *J. Chem. Phys.* **2008**, 128, 114510.
- (52) Tanaka, F.; Ishida, M.; Matsuyama, A. *Macromolecules* **1991**, 24, 5582.
- (53) Tanaka, F.; Ishida, M. *Macromolecules* **1997**, 30, 1836.
- (54) Dormidontova, E.; Ten Brinke, G. *Macromolecules* **1998**, 31, 2649.
- (55) Angerman, H. J.; Ten Brinke, G. *Macromolecules* **1999**, 32, 6813.
- (56) Dudowicz, J.; Freed, K. F. *Macromolecules* **2000**, 33, 5292.
- (57) Huh, J.; Jo, W. H. *Macromolecules* **2004**, 37, 3037.
- (58) Takano, A.; Soga, K.; Asari, T.; Suzuki, J.; Arai, S.; Saka, H.; Matsushita, Y. *Macromolecules* **2003**, 36, 8216.
- (59) Takano, A.; Soga, K.; Suzuki, J.; Matsushita, Y. *Macromolecules* **2003**, 36, 9288.
- (60) Jaffer, K. M.; Wickham, R. A.; Shi, A.-C. *Macromolecules* **2004**, 37, 7042.
- (61) Panyukov, S. V.; Rabin, Y. *Phys. Rep.* **1996**, 269, 1.
- (62) Panyukov, S. V.; Rabin, Y. In *Theoretical and Mathematical Methods in Polymer Research*; Grosberg, A. Y., Ed.; Academic Press: New York, 1998.